M.tb diminishes SARS-CoV-2 severity through innate immune priming

Brittany D. Williams

A dissertation

submitted in partial fulfillment of the

requirements for the degree of

Doctor of Philosophy

University of Washington

2024

Reading Committee:

Rhea N. Coler, Chair

Thomas Hawn

Jennifer Hyde

Program Authorized to Offer Degree:

Pathobiology

University of Washington

Abstract

M.tb diminishes SARS-CoV-2 severity through innate immune priming

Brittany D. Williams

Chair of the Supervisory Committee:

Rhea N. Coler

Department of Global Health

Early in the coronavirus disease 2019 (COVID-19) pandemic, individuals with chronic lung conditions, including tuberculosis (TB), were recognized to be at elevated risk for severe COVID-19 outcomes. Despite this concern, clinical studies have reported inconclusive evidence regarding the specific risks SARS-CoV-2 poses to the over 10 million individuals infected with Mycobacterium tuberculosis (M.tb). M.tb infection is well-characterized by a persistent, robust proinflammatory immune response within the lung parenchyma, predominantly driven by IFNγ and T helper 1 (Th1) responses. IFNγ is known for its antiviral properties and its ability to activate a range of interferon-stimulated genes (ISGs) in various cell subsets, including epithelial cells. Therefore, we hypothesized that primary infection with M.tb would induce an immune response, characterized by elevated IFNγ levels, that promotes the transcription of ISGs, creating an antiviral environment that primes the lung to better restrict viral replication upon secondary infection with SARS-CoV-2.

Our study aims to dissect the complex interactions between M.tb and severe acute respiratory syndrome coronavirus 2 (SARS-CoV-2) in a co-infection model, focusing on how the innate immune response induced by M.tb can modulate viral replication. To investigate this, we developed an M.tb and SARS-CoV-2 co-infection model utilizing transgenic K18-hACE2 mice. Mice were first infected with a low-dose aerosol of M.tb HN878, followed by intranasal infection with a sublethal dose of SARS-CoV-2 variant Beta. We then conducted an in-depth characterization of the co-infection model and employed mechanistic *in vitro* assays to evaluate the dynamics of the immune response. Our investigation centered on the role of cytokine-mediated signaling in lung epithelial cells, particularly how these signals trigger the upregulation of antiviral genes that serve as a preemptive defense against SARS-CoV-2. Our findings reveal that IFNγ induced by M.tb infection is pivotal in activating antiviral pathways within lung epithelial cells, thereby limiting viral replication and reducing the overall severity of SARS-CoV-2 infection. We have identified key immune responses that play a critical role in this protective response, highlighting potential therapeutic targets that could be exploited to enhance antiviral immunity in the context of co-infection.

In all, this study provides an analysis of the immune pathways activated by a pre-existing bacterial M.tb infection that confer protection against SARS-CoV-2. By identifying the molecular players involved, our research offers novel insights into potential therapeutic strategies of IFNγ that could be harnessed to mitigate the impact of COVID-19, particularly in populations with high TB burden.

TABLE OF CONTENTS

LIST OF FIGURES

LIST OF TABLES

ACKNOWLEDGEMENTS

This work could not have been accomplished without the guidance and never-ending support from my mentor, Dr. Rhea Coler. Through the trials and tribulations, Rhea has remained steadfast in her belief in me. I have come out of my graduate studies twice the scientist than when I began, and I thank you immensely for this. In extension, I would like to acknowledge the pillars of the Coler lab, Dr. Susan Baldwin, Dr. Sasha Larsen Akins and Tiffany Pecor for training me to be a strong, efficient, and well-organized scientist. It has been great to have strong yet so kind woman scientist to look up to. I must also thank my fellow Coler lab members for always providing their expertise, time, and optimism to this thesis work. The long hours in the BSL3 would have been impossible without this team's kind and always entertaining support.

I would also like to acknowledge my committee, Dr. Tom Hawn, Dr. Jenny Hyde, Dr. Kristina Adams-Waldorf, and Dr, Whitney Harrington, for taking the time to guide me through this thesis and pushing me to be a better scientist. A big thank you to the Pathobiology program for getting me to this point, and although we are small we are mighty.

DEDICATION

I would like to dedicate this thesis to my family for always supporting me and believing in me. As a first-generation college student, I have been privileged to take this time to study and train to become a better scholar and scientist—an opportunity that wouldn't have been possible without the sacrifice and hard work of my parents, Maria and Anthony Williams. They taught me to be kind, to believe in the glory of God, to always work hard and to never give up.

My time in Seattle has been made worthwhile by the amazing people I have met while here. My biggest supporter and cheerleader, Kaleb, thank you for everything you've done for me through this journey. Thank you for pushing me every day to keep going and encouraging me to keep getting up even after I fall. It was far from easy, but we have only come out stronger.

To my dear amazing friends, thank you for always forcing me to have fun and to take a break. The smartest and kindest people there is and so thankful to have met you all. I am excited to see all the great things you continue to accomplish. You inspired me to keep going and to remember although the Ph.D. journey is hard, it will be worth it in the end.

CHAPTER 1. INTRODUCTION

1.1 TB Prevalence and history

Tuberculosis (TB) is a long-standing chronic infectious disease. Until the emergence of coronavirus disease 2019 (COVID-19), TB was the leading infectious disease killer globally (1). Despite centuries of efforts to combat TB, it continues to claim millions of lives each year, with an estimated 1.3 million TB-related deaths recorded in 2022 (2).

The causative agent of TB, Mycobacterium tuberculosis (M.tb), was discovered in 1882 by Dr. Robert Koch, who identified it in infected tissues. This groundbreaking discovery earned Dr. Koch the Nobel Prize in Medicine in 1905. Although M.tb was not identified until the 19th century, TB is known to be an ancient disease, with evidence of cases dating back to ancient Egypt (3, 4). Throughout history, TB has been documented globally under various names, including "phthisis" in ancient Greece, "the white plague" in the 1700s, and "consumption" in the 1800s (3).

The identification of M.tb marked a significant milestone in medical science. Dr. Koch employed a novel staining technique, akin to the one used for identifying the leprosy bacillus, another Mycobacterium discovered around the same time. This discovery was pivotal, as TB was responsible for one in seven deaths globally during that period (3).

Given its ancient origins, many questions remain about the origins and evolution of TB. The Mycobacterium genus encompasses over 170 species, many of which are environmental bacteria (5). Among these, three major species are known to cause significant diseases in humans: *Mycobacterium leprae* (leprosy), *Mycobacterium ulcerans* (Buruli ulcer), and the Mycobacterium tuberculosis complex (MTBC) (5).

The MTBC includes over 10 bacteria species that are genetically similar, rod-shaped acid-fast bacilli, which primarily infect macrophages and capable of causing the chronic bacterial infection, TB, in various hosts (6). This group includes M.tb, *Mycobacterium bovis, Mycobacterium africanum*, and *Mycobacterium caprae*, with M.tb being the primary cause of TB in humans (6).

Given MTBC species have coexisted with humans and animals for centuries the evolution of the species is still not well known and believed to have evolved with human migration (7). Within the M.tb group, there are nine recognized lineages with lineages 1-4 being widely distributed globally, therefore labeled as generalists (8-10).

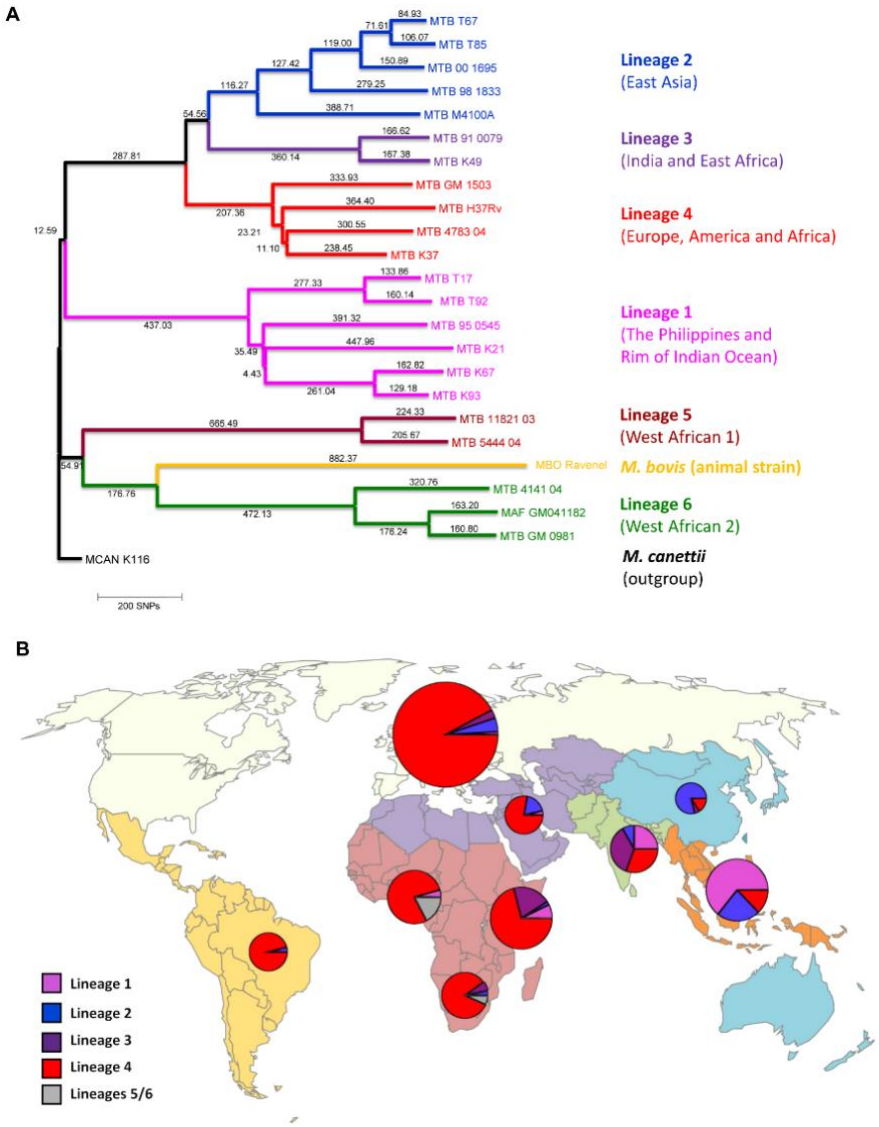

Figure 1.1. *M.tb lineages. Lineages of M.tb are distributed globally, with lineages 1-4 being the most widely distributed globally.* ***Figure 1.1*** *was reproduced from (11) (Lucas Fenner) with permission, Creative Commons Attribution-NonCommercial-ShareAlike 4.0 International License.*

1.2 TB pathology and host response

M.tb is transmitted through aerosol droplets produced by individuals with active infection (12). Upon inhalation, the bacilli travel through the upper respiratory tract to reach the alveoli in the lower respiratory tract. There, they first encounter alveolar macrophages (AMs). M.tb is phagocytosed by AMs using various receptors, including complement receptors (CR), the mannose receptor (MR), surfactant molecules, and dendritic cell-specific intracellular adhesion molecule-3–grabbing nonintegrin (DC-SIGN) (13, 14). AMs also detect M.tb through multiple pattern recognition receptors (PRRs), including C-type lectin receptors (CLRs), Nod-like receptors (NLRs), and Toll-like receptors (TLRs) 2, 4, and 9 (15-18). The uptake of M.tb and the subsequent activation of AMs facilitate the elimination of the bacteria by producing nitric oxide and reactive oxygen species (ROS) (19, 20). This process also promotes pro-inflammatory responses through the production of cytokines and chemokines, such as interleukin-6 (IL-6), tumor necrosis factor-alpha (TNF-α), and interleukin-12 (IL-12) (13, 21, 22). Despite these efforts, M.tb can create a niche within phagocytic cells to avoid elimination by utilizing multiple mechanisms. These include going dormant to avoid detection, inhibiting phago-lysosome fusion, and reducing the production of ROS (22-24). Once engulfed, alveolar macrophages travel to the lung interstitium, where they can further recruit other innate immune cells, including dendritic cells, natural killer (NK) cells, monocytes, and neutrophils (25). The slow replication rate of M.tb, with a doubling time of approximately 24 hours, delays the host's ability to effectively detect the bacteria (26). As a result, an M.tb-specific T-cell response is not activated until around 14 days post-infection and peaks 3-4 weeks post-infection (27).

The T-cell response is crucial in combating M.tb infection. This is evident in HIV-positive patients, who, due to depleted CD4 T-cell reservoirs, are at high risk for TB (28). Mouse and non-human primate (NHP) studies have shown that depletion of CD4 T cells increases the severity of M.tb infection (29-32). As an intracellular pathogen, M.tb predominantly elicits a Th1 CD4 T cell

response. A robust Th1 response, characterized by the production of key effector cytokines IL-12 and IFNγ, is essential for activating infected macrophages to effectively clear M.tb and contain the infection (33). Recent studies, however, have highlighted the importance of early induction of proinflammatory Th17 responses to promote cell recruitment and granuloma formation in hopes of controlling the infection (33). Although, a balance of Th1 and Th17 responses is needed. If responses are skewed towards Th17 it can result in elevated neutrophil requirement and tissue damage (34).

At this stage, complete elimination of M.tb infection is possible and nearly 90% of infected individuals successfully eliminate or contain infection (35, 36). However, in some individuals, the infection persists due to M.tb-induced necrosis of infected macrophages, which allows M.tb to be released and target recruited phagocytic cells, such as macrophages and dendritic cells (37). This leads to increased M.tb replication and the initiation of granuloma formation (37). While it remains unknown why some individuals can eliminate the infection while others progress to granuloma formation, the granuloma represents the host's immune response to contain the infection. While the structure of the granuloma can evolve, it can consist of M.tb bacilli and infected macrophages at its core, surrounded by epithelioid and foamy macrophages, and other innate immune cells (38-40). Encircling these are lymphocytes, forming a lymphocytic cuff composed of B and T cells (38-40). Successful containment within the granuloma can result in a reduced number of bacilli in the lungs, rendering the infection latent (41). It is estimated that approximately one-fourth of the world's population is latently infected with M.tb (42). Although individuals with latent TB are asymptomatic and non-contagious, M.tb can persist within the granuloma (41). Any alterations in the immune system, such as taking immunosuppressants, can compromise containment and reactivate the infection. As the infection progresses, the granuloma core can become caseous, with an increase in foamy macrophages and necrotic host immune cells (12). In late-stage TB, cavitation of the granuloma allows the bacilli to spread to other areas of the lung. At this stage of

active TB disease, the infected individual can transmit the bacilli to new hosts, initiating a new infection cycle (12).

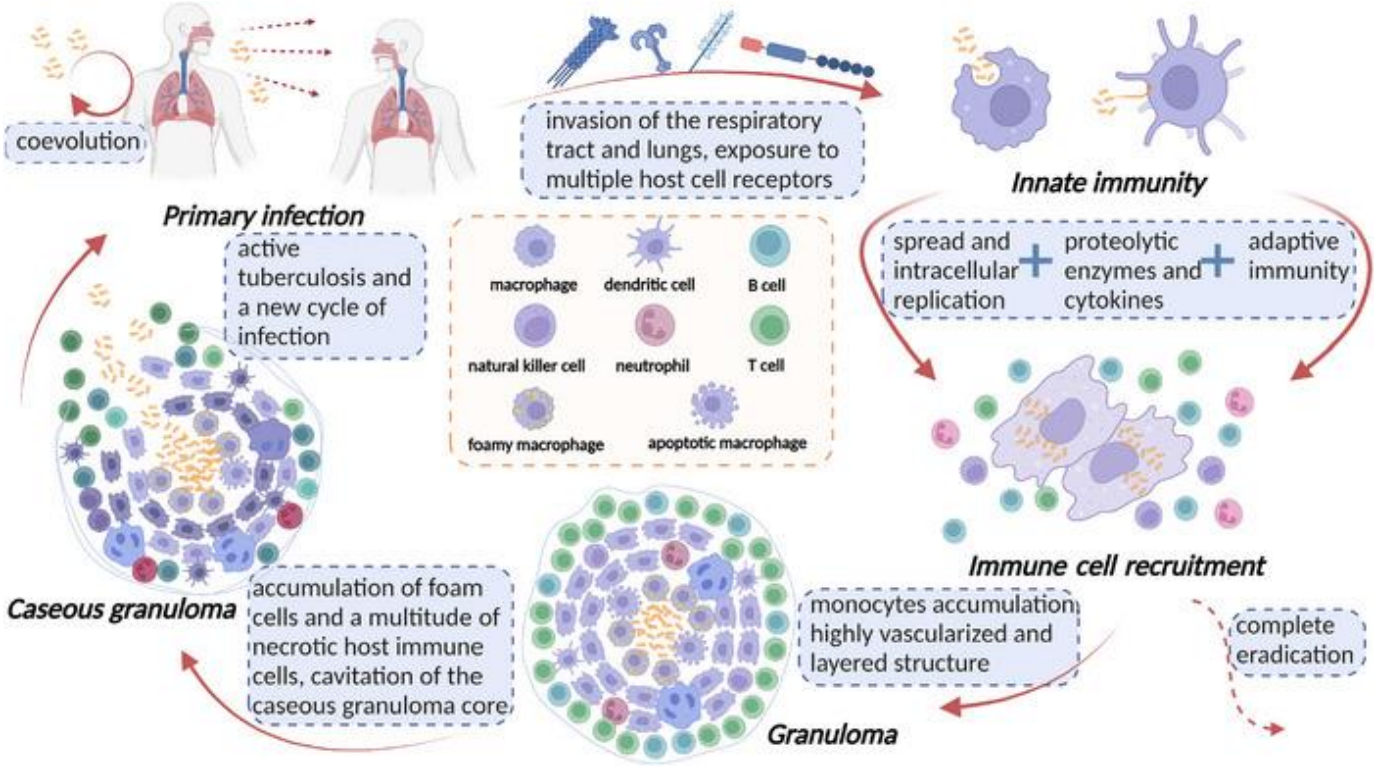

Figure 1.2. *M.tb pathogenesis. M.tb infection leads to a spectrum of infection and disease outcomes. M.tb infection in the lungs will induce a robust innate response, followed by T and B cell recruitment to the site of infection forming a granuloma. In 90% of individuals, infection can be successfully eliminated or contained. However in the 10% of individuals infection will progress to necrosis of the granuloma and active TB disease.* ***Figure 1.2*** *was reproduced from (12) (Jiaxing Yang) with permission, Creative Commons Attribution-NonCommercial-ShareAlike 4.0 International License.*

1.3 SARS-CoV-2 emergence

The emergence of severe acute respiratory syndrome coronavirus 2 (SARS-CoV-2) in Wuhan, China, during the winter of 2019 rapidly escalated into the COVID-19 pandemic, claiming over 6.8 million lives by March 2023 (43). Initially, the cause of the mysterious pneumonia-like cases in Wuhan was unknown. By January 2020, the Chinese Center for Disease Control and Prevention isolated the novel coronavirus from a patient swab (44). A month later, the International Committee on Taxonomy of Viruses officially named the virus "SARS-CoV-2" and

by March 2020 with cases in over 200 countries the World Health Organization (WHO) declared COVID-19 a pandemic (45, 46).

While there has been controversy surrounding the origins of SARS-CoV-2, it is widely held the virus was initially spread at a market in Wuhan via zoonotic transmission (45). Bats, known natural hosts of many coronaviruses, are postulated to have transmitted the virus to an intermediate animal present at the market (45). SARS-CoV-2 is the 7th documented Coronavirus zoonotic spillover and the third case of severe disease in humans, the other two being the SARS-CoV epidemic in 2002 and Middle East Respiratory Coronavirus (MERS-CoV) in 2012 (47).

There are hundreds of viruses within the coronavirus family. The viruses are categorized into four subgroups based on genome sequences and serological response, including Alpha-, Beta-, Gamma-, and Delta-coronaviruses, with SARS-CoV, MERS-CoV and SARS-CoV-2 belonging to the betacoronavirus genera (48, 49). The first coronavirus was first isolated in 1937 and identified to be the cause of bronchitis in poultry (48, 50, 51). Though the characterization of human respiratory coronaviruses wouldn't be until the 1960s (50, 52). Most of the coronaviruses were known to cause disease within animals and tend to be non-lethal or lead to the common cold in humans such as HCov NL63 and HKU1 (50). The recent outbreaks involving SARS-CoV in 2003, MERS-CoV in 2012 and SARS-CoV-2 in 2019 did alarm the public to the potential of coronaviruses to spillover to humans and cause devasting events (48).

SARS-CoV-2 and other coronaviruses derive their name from their crown-like appearance on the surface. SARS-CoV-2 is a positive single-stranded RNA (+ssRNA) enveloped virus with a genome size of approximately 30kb (53). It comprises four major structural proteins: spike (S) protein, envelope (E) protein, membrane (M) protein, and nucleocapsid (N) protein (53). These proteins are essential for virion assembly and are believed to suppress the host immune response (53, 54). Additionally, SARS-CoV-2 encodes polyproteins pp1a and pp1b, which are processed into 16 nonstructural proteins (NSPs) necessary for viral replication and transcription (54). The

virus also encodes 11 accessory proteins that, while not essential for replication, assist in viral replication by modulating host immune responses (54).

A significant issue that arose during the pandemic was the rapid emergence of SARS-CoV-2 variants. Early in the pandemic, a single spike protein substitution, D614G, quickly became prevalent, conferring a selective advantage (55). While this variant was not associated with increased severity, it was linked to higher viral loads and a broader age range of infected patients (55, 56). Subsequently, numerous variants continued to emerge. By December 2021, the WHO had identified five SARS-CoV-2 variants of concern (VOCs): Alpha (B.1.1.7), Beta (B.1.351), Delta (B.1.617.2), Gamma (P.1), and Omicron (B.1.1.529) (57-61). These VOCs possessed multiple mutations throughout their genomes, particularly in the receptor binding domain (RBD), raising significant concerns (57). The N501Y mutation in the RBD, first noted in the Alpha and Beta VOCs, increased the spike protein's affinity for the ACE2 receptor, resulting in enhanced cellular entry (57). The emergence of the Delta variant underscored that mutations in the RBD, a target for neutralizing antibodies, could reduce the efficacy of antibodies generated by natural infection or vaccination, thereby decreasing vaccine effectiveness (57). Despite extensive efforts to contain SARS-CoV-2's spread and the rapid deployment of mass vaccination plans, emerging variants continue to pose global challenges.

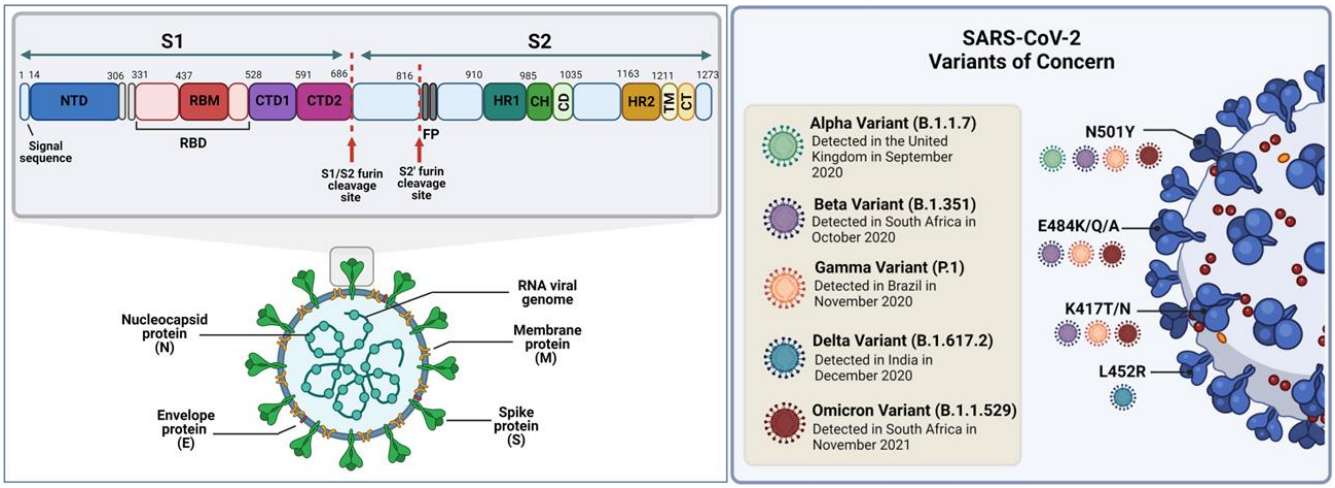

***Figure 1.3**. SARS-CoV-2 structure and VOCs. **Figure 1.3** was reproduced from* (62) *(Priyal Mistry) with permission, Creative Commons Attribution-NonCommercial-ShareAlike 4.0 International License.*

1.4 SARS-CoV-2 pathology and host response

Early in the pandemic, it became evident that the virus was spreading rapidly and could cause a wide range of disease outcomes, from asymptomatic cases to severe acute respiratory distress syndrome (ARDS) and multi-organ failure (63). Alarmingly, large populations were identified as being at risk for severe disease. The Centers for Disease Control and Prevention (CDC) identified common risk factors for severe viral infections, such as old age and immunocompromised states (64). Surprisingly, many individuals with chronic diseases were also at high risk. These chronic conditions included obesity, heart disease, diabetes, kidney disease, liver disease, cerebrovascular disease, and chronic lung disease (64).

SARS-CoV-2 is predominantly transmitted via aerosol droplets, which can be spread by an infected person coughing (65, 66). Contact tracing has also identified that the risk of transmission correlates with proximity to an infected individual (65, 67, 68). Once inhaled, SARS-CoV-2 first encounters the upper respiratory tract, specifically targeting multi-ciliated airway cells in the nasopharynx and trachea that express the entry receptor angiotensin-converting enzyme-2 (ACE2) (69). Successful induction of antiviral immune responses driven by type I interferon (IFN), followed by B and T cell responses, can clear the infection, resulting in only mild cold-like symptoms (69). However, if the immune response is inadequate, SARS-CoV-2 can travel along the tracheobronchial tree to the lower respiratory tract. Once the virus reaches the alveoli, it can cause more severe infection by targeting alveolar type 2 (AT2) cells, which secrete pulmonary surfactants needed to lubricate the lungs and serve as progenitor cells for alveolar type 1 (AT1) cells (69, 70).

The S1 region of the SARS-CoV-2 spike protein binds to the host ACE2 receptor. Upon binding, the host protease cleaves the spike protein, exposing the S2 region. The activated S2 region then fuses the viral envelope with the host lipid bilayer and deposits its +ssRNA into the host cell and the viral replication process can begin (69). Alternatively, SARS-CoV-2 can enter

the host cell via clathrin-mediated endocytosis, where the spike protein is cleaved by cathepsins, non-specific proteases (71).

Once inside the cell, SARS-CoV-2 can be detected by pattern recognition receptors (PRRs), activating the host immune response. The retinoic acid-inducible gene-I (RIG-I)-like receptor (RLR) family, particularly melanoma differentiation-associated protein 5 (MDA5), which detects long double-stranded RNAs (dsRNAs) within the cytoplasm, has been identified as the primary sensor (69, 72). Another RLR, RIG-I, has been identified as a restriction factor (73). Other potential PRRs include Toll-like receptors 3 (TLR3) and 4 (TLR4) (69). Upon activation, MDA5 binds to viral material and initiates signaling through the mitochondrial antiviral signaling protein (MAVS) pathway to induce the transcription of type I and III IFNs. Utilizing both autocrine and paracrine signaling IFNs can induce interferon-stimulated genes (ISGs) that promote an antiviral state through various mechanisms. Additionally, bystander epithelial cells and innate immune cells, such as neutrophils and macrophages, can further produce IFNs and cytokines to help control the infection. An adequate innate response can promote the development of B and T cell responses, which are crucial for eliminating the virus (69). However, SARS-CoV-2 has developed numerous mechanisms to hinder various aspects of the immune response. Notably, through its ability to evade and hinder the innate immune response SARS-CoV-2 infection has been characterized by inducing low innate antiviral defenses, with low levels of type I and III IFNs, compared to other respiratory viruses (74).

Upon translation of its viral genomic RNA, SARS-CoV-2, like other coronaviruses, undergoes capping and methylation of its genomic RNA and sub genomic RNA to ensure successful interaction with host ribosomes and to evade host detection (75). Additionally, to avoid detection of intermediate double-stranded RNAs (dsRNAs), SARS-CoV-2 utilizes nonstructural protein 15 (NSP15) through its endonuclease activity to reduce the amount of negative-stranded RNA and dsRNA (75). It also employs double-membrane vesicles (DMVs) during replication (75). SARS-CoV-2 deploys various strategies to hinder the host innate immune response, including

blocking PRR activation, MAVS activity, NF-κB and IRF3 signaling, and type I IFN signaling (75-77). By inhibiting the innate response, the virus can replicate without significant detection or challenge from the host immune system. The resulting large viral load can lead to increased death of alveolar type 2 (AT2) cells, causing alveolar damage and generating large amounts of pathogen-associated molecular patterns (PAMPs) and damage-associated molecular patterns (DAMPs). The delayed response coupled with large amounts of PAMPS and DAMPS can promote a dysregulated immune response, cultivating systemic hyperinflammation, known as a cytokine storm (78). This hyper proinflammatory response, seen in severe COVID-19 patients, is characterized by an absence of IFN responses and elevated levels of granulocyte colony-stimulating factor (G-CSF), IP-10, MCP-1, macrophage inflammatory protein 1α (MIP-1α), TNF-α, IL-2, IL-6, IL-7, IL-10 (74, 78). The resulting inflammation can induce lung injury such as edema, fibrosis, and thrombosis which can progress to hypoxia, ARDS, and death (78).

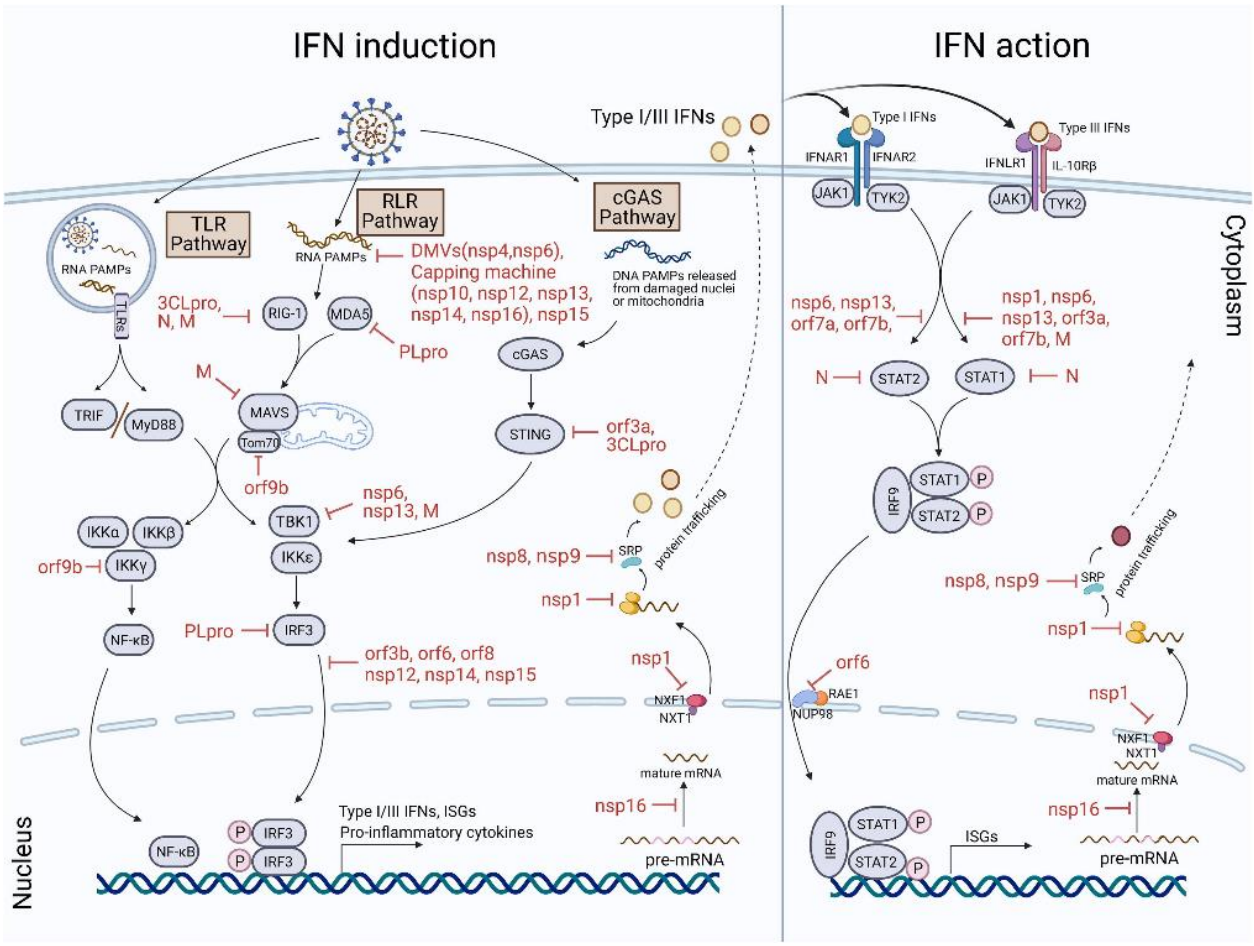

Figure 1.4. *SARS-CoV-2 immune evasion.* ***Figure 1.4*** *was reproduced from* (79)*(Yuan-Qin Min) with permission, Creative Commons Attribution-NonCommercial-ShareAlike 4.0 International License.*

1.5 SARS-CoV-2 and M.tb co-infection clinical findings

The CDC declared chronic lung diseases as a risk factor early in the COVID-19 pandemic, raising concerns for the 10 million people with TB. Given the prevalence of both TB and COVID-19, co-infections were anticipated. Initial clinical findings on TB and COVID-19 co-infections began to emerge at the start of the pandemic.

An observational case-control study involving three primary care hospitals in Shenyang, China, reported that M.tb infection likely increases susceptibility to SARS-CoV-2 with M.tb infection being more prevalent in COVID-19 patients compared to bacterial and viral pneumonia patients (36.11% vs 20% and 16.13%) (80). Additionally, M.tb co-infection cases had a larger percentage of severe COVID-19 compared to mild COVID-19 symptoms (78% vs 22%), with

severe COVID-19 classified by lymphopenia, dyspnea and ARDS development (80). However, the study included only 36 patients and noted that its findings require validation in a larger study. Similarly, a population cohort study using data from adults attending public-sector health facilities in Western Cape, South Africa, found that patients with both previous and current TB had increased COVID-19 mortality compared to those without TB (adjusted hazard ratios of 2.70 for co-infected patients and 1.51 for non-TB patients) (81). Unlike the Shenyang study, this study had a larger cohort of over 3 million patients. However, it mentioned that residual confounding factors due to HIV and TB co-infections could result in an overestimation of HIV- and TB-associated COVID-19 mortality risks. In contrast, a retrospective cohort study in an Indonesian tertiary lung hospital including 1034 confirmed COVID-19 patients reported TB co-infection was negatively associated with COVID-19 mortality (82). TB co-infected patients exhibited a lower estimated death rate than the COVID-19 only group (6.5 vs. 18.8 per 1000 population) (82). Additionally, a prospective study on those with latent TB infection (LTBI) and COVID-19 in India found LTBI prevalence was lower in severe compared to non-severe COVID-19 patients (4% vs 40%) (83). As noted in other studies, the study does have a small cohort size of 15 patients and does require a larger study to validate their results. Another prospective study conducted at a hospital in Northern Italy following in-patients with TB overall found TB and COVID-19 co-infection was generally benign and with proper care is clinically manageable (84). However, once again due to a cohort size of 20 patients the findings would need to be confirmed in a larger cohort study. While clinical studies provide valuable insights into co-infection outcomes in patients, they also face challenges such as small cohort sizes, potential confounding factors due to comorbidities, and unknown infection timelines. These limitations underscore the potential of pre-clinical studies to offer a more controlled environment for investigating the specific interactions between M.tb and SARS-CoV-2.

1.6 Bacteria and virus co-infections

When predicting the outcomes of M.tb and SARS-CoV-2 co-infection, one can evaluate previous incidences of M.tb and viral co-infections. A notable example is the co-infection of TB and human immunodeficiency virus (HIV), which remains a pressing issue. According to the WHO, 167,000 TB-related deaths occurred in 2023 among individuals who are HIV-positive (2). This dual infection creates a "perfect storm," where HIV significantly contributes to the progression of TB disease in individuals who are latently infected with M.tb. Additionally, HIV co-infection exacerbates TB disease, primarily due to the depletion of CD4+ T cells, which are critical for the immune response against TB. Conversely, TB infection can promote HIV replication, accelerating the progression of HIV to acquired immunodeficiency syndrome (AIDS), further complicating the clinical management of both diseases (28). This bidirectional potentiation underscores the need for integrated treatment approaches to manage TB-HIV co-infections effectively.

However, not all TB co-infections exhibit such synergistic interactions. For instance, the outcomes of TB and influenza co-infections are less definitive and can vary depending on the timing and sequence of infections. A systematic review of clinical studies investigating co-infections of influenza A virus (IAV) and M.tb found the association between co-infection and exacerbated disease outcomes to be inconclusive (85). In preclinical models, Redford et al. demonstrated that exposure of mice to IAV prior to or concurrently with M.tb H37Rv infection resulted in decreased survival and increased bacterial burden, potentially mediated by induced type I IFN signaling (86). Notably, the study also revealed that bacterial load increased with co-infection with two IAV subtypes (H3N2 and H1N1) but not with one IAV subtype (H1N1). Further, a study involving initial M.tb H37Rv infection in mice followed by co-infection with IAV (H1N1) 12 days later reported increased bacterial loads and reduced survival. IAV which induces increased IL-10 is suggested to compromise the control of M.tb infection by dampening the activated proinflammatory response (87). Unfortunately, these studies do not report viral burden outcomes and whether co-infection can exacerbate the viral infection. However, Kaufmann et al. showed that Bacille Calmette-Guérin (BCG) TICE immunization administered intravenously followed by

IAV (H1N1) infection four weeks later resulted in increased survival and decreased viral load (88). This effect may be attributed to trained immunity, allotting monocytes from BCG-immunized mice to mount a rapid and efficient cytokine response to IAV.

In summary, while clinical data on M.tb and IAV co-infections remain inconclusive, preclinical studies indicate that such co-infections lead to worsened TB outcomes in mice. This effect is potentially driven by type I IFN responses that antagonize the IFNγ responses crucial for TB control, as well as IL-10 production, which can impair the immune response to M.tb infection. Given these findings, it would be interesting to investigate whether the lower type I IFN response observed in SARS-CoV-2 infection might mitigate the exacerbation of TB disease that's seen in these preclinical IAV and M.tb studies. Moreover, the protective effect of BCG immunization against IAV infection is notable, especially since early in the COVID-19 pandemic, there was significant interest in whether BCG immunization could provide protection against SARS-CoV-2.

BCG is a live attenuated vaccine derived from *Mycobacterium bovis* and was first utilized for human immunization in 1921. To this day, it remains the only officially licensed vaccine against M.tb. Despite its highly variable efficacy in preventing pulmonary TB disease or reactivation, BCG is widely employed in newborn immunization programs in TB-endemic regions due to its proven protection against disseminated or miliary TB and TB meningitis in young children (89). Recent investigations have focused on the off-target effects of BCG, particularly its ability to induce trained immunity (90). One study assessed BCG-immunized healthcare workers and found that BCG immunization was associated with decreased SARS-CoV-2 IgG seroconversion (91). Additionally, healthcare workers with a history of BCG immunization self-reported fewer COVID-19 symptom (91). However, the study acknowledged the need for larger randomized clinical trials to validate these results. In response to these findings, a double-blind, placebo-controlled trial was conducted in which healthcare workers received either the BCG-Denmark vaccine or a saline placebo, with COVID-19 outcomes being assessed (92). This trial reported that BCG immunization did not result in a lower risk of COVID-19 compared to the placebo (92).

In animal studies, Kaufmann et al. investigated the impact of BCG immunization on SARS-CoV-2 outcomes by administering BCG-TICE either intravenously or subcutaneously to mice, followed by SARS-CoV-2 challenge 4 weeks post immunization (88). Their findings indicated no significant differences in viral loads or survival between immunized and non-immunized mice (88). Conversely, Hilligan et al. reported that mice immunized intravenously, but not subcutaneously, with BCG Pasteur and challenged with SARS-CoV-2 6 weeks post-vaccination exhibited increased survival and decreased lung viral loads compared to intravenous (i.v.) PBS control-treated BCG subcutaneous (s.c.)-immunized mice (93). An additional study, which immunized mice with BCG Tokyo-172 strain intravenously and challenged mice with SARS-CoV-2 45-days post-immunization, also measured decreased lung viral burden and increased protection in BCG immunized mice, validating the protective effects of BCG in the preclinical model (94). The discrepancy in outcomes between the studies may be attributable to the different BCG strains utilized and timing of BCG immunization.

Hilligan et al. further observed that BCG-immunized mice displayed modified inflammatory responses, characterized by decreased levels of proinflammatory cytokines and increased accumulation of resident interstitial myeloid cells in the lungs, compared to i.v. PBS-treated and BCG s.c. immunized mice (93). The authors proposed that prior intravenous BCG administration might mitigate the detrimental inflammatory effects of SARS-CoV-2 through BCG-induced IFNγ effects on lung epithelial and myeloid cells, underscoring the potential for innate immune priming to confer nonspecific protection against SARS-CoV-2.

While preclinical studies have demonstrated a beneficial relationship between BCG immunization and improved SARS-CoV-2 outcomes, the impact of an active M.tb infection on co-infection outcomes with SARS-CoV-2 remains an open question. Given the observed protective effects of BCG, we hypothesize that an ongoing M.tb infection could similarly prime the immune system, leading to a protective effect. This hypothesis suggests that the active immune response within the lungs during an M.tb infection may enhance the host's ability to combat SARS-CoV-2,

potentially replicating the protective phenotype seen with BCG immunization. Further comprehensive research is essential to elucidate the dynamics and clinical implications of such co-infection fully.

1.7 Mechanism of protective phenotype remain to be identified

It is well known an efficient initial innate immune response, particularly the type I IFN response, is crucial for combating SARS-CoV-2 infection. Insufficient activation of this response can lead to a dysregulated immune reaction, where the innate response becomes more harmful than protective (95).

IFNs are a group of cytokines that include type I, II, and III IFN families. Type I IFNs, which include IFN-α and IFN-β, and the increasingly recognized type III IFNs (e.g., IFN-λ), are traditionally associated with antiviral responses (95). Type I IFNs exert their effects by binding to a heterodimeric receptor composed of IFNAR1 and IFNAR2 subunits. This binding activates Janus kinase 1 (JAK1) and tyrosine kinase 2 (TYK2), which phosphorylate and activate signal transducer and activator of transcription (STAT) proteins, leading to the formation of the ISG factor 3 (ISGF3) complex. The ISGF3 complex, composed of STAT1, STAT2, and IRF9, then translocate to the nucleus, where it binds to the IFN-stimulated response element (ISRE) within the promoters of interferon-stimulated genes (ISGs). This binding promotes the transcription of a broad range of ISGs that mediate antiviral responses (96).

The ISGs can employ multiple mechanisms to restrict viral activity, including inhibiting viral replication, degrading viral RNA, and enhancing antigen presentation to T cells (96). For example, ISGs such as MX1, OAS, and PKR can inhibit various stages of the viral life cycle, while ISG15 and ISG20 can degrade viral components and modulate immune signaling pathways (96). Type I IFNs also play a role in modulating the immune response beyond direct antiviral activities. They can enhance the activation and maturation of dendritic cells, promote the differentiation of Th1 cells, and stimulate the cytotoxic activity of NK cells (96). Additionally, type I IFNs can induce

the expression of chemokines that recruit immune cells to sites of infection, thereby orchestrating a coordinated immune response.

However, type I IFNs have a complex and sometimes detrimental role in M.tb infection due to their antagonistic relationship with IFNγ. Type I IFNs can downregulate the IFNγ receptor (IFNGR) on macrophages, impairing the IFNγ signaling pathway (97). Type I IFNs can be induced during M.tb infection, potentially through the cGAS-STING and TLR9 signaling pathways, but their levels can vary depending on the M.tb strain and animal model used (98). In contrast, IFNγ, primarily produced by NK cells, CD8 cytotoxic T cells and CD4 Th1 cells, plays a critical role in TB immunity (99). While IFNγ is well-known for its role in activating macrophages and the cell-mediated immune response, its antiviral capabilities are less frequently highlighted.

IFNγ activates signaling by binding to the heterodimeric IFNGR1-IFNGR2 receptor, which is ubiquitously expressed on various cell types including immune cells and epithelial cells (100). IFNGR can also be upregulated by proinflammatory cytokines, TNF-α and IL-1 (101, 102). Upon binding to IFNGR, JAK1 and JAK2 are recruited then phosphorylated (102). The phosphorylated proteins subsequently recruit and phosphorylate STAT1 homodimers which then translocate to the nucleus to bind IFNγ-activated site (GAS) elements to promote transcription of ISGs (102). Like type I and III IFNs, the ISGs induced by IFNγ include a broad range of activities. Indeed, while IFNγ can induce a unique set of ISGs it does share many ISGs with type I IFN that could create an antiviral environment and provide protection against a virus such as SARS-CoV-2 (97). Known antiviral ISGs induced by IFNγ include the aforementioned OAS, MX1, ISG15, ISG20 many interferon regulatory factors (IRFs) vital to many immune signaling cascades, and the PRRs Ddx58 (RIG-I) and IFIH1 (MDA5), among many others (103).

Given M.tb infection leads to robust and abundant IFNγ production within the lung, we can infer it will not only work to activate macrophages but also act upon many cells to induce ISG production. In the context of M.tb and SARS-CoV-2 co-infection in which there is an initial and established M.tb infection, we hypothesize this established immune response comprised of IFNγ

can prime the lung environment to induce ISG expression in bystander epithelial cells so upon secondary infection with SARS-CoV-2 these epithelial cells targeted by SARS-CoV-2 will have already been alerted to an infection and be able to overcome SARS-CoV-2's ability to evade and hinder the immune response during the crucial first moments of infection measured through decreased viral loads and increased protection.

1.8 Summary

I have described above the emergence and respective immune responses of two globally prevalent pathogens, M.tb and SARS-CoV-2 which pose a risk for millions. However, it remains unclear how co-infection would affect disease outcome. M.tb infection induces a complex and robust immune response characterized by a diverse innate response and Th1 response with importance of IFNγ production needed to combat infection. M.tb infection is also unique in that it can progress to a chronic infection in which recruited immune cells remain within the lung and can form a granuloma to contain the infection. While SARS-CoV-2 infection deploys mechanisms to evade and hinder the initial immune response, which can aid in the virus being able to replicate uncontrollably prior to detection. Clinical characterizations of patients have also shown that those with early IFN (type I-III) responses had less severe cases of COVID-19 (104). In the context of M.tb and SARS-CoV-2 co-infection, having established M.tb infection and an extensive immune response in the lung prior to secondary infection with SARS-CoV-2 may provide a primed environment that can overhaul SARS-CoV-2's ability to avoid detection and therefore decrease initial viral replication overload. Given the complications in clinical studies, building a preclinical mouse model we may be able to further investigate M.tb and SARS-CoV-2 infection in a controlled environment and further elucidate this proposed hypothesis.

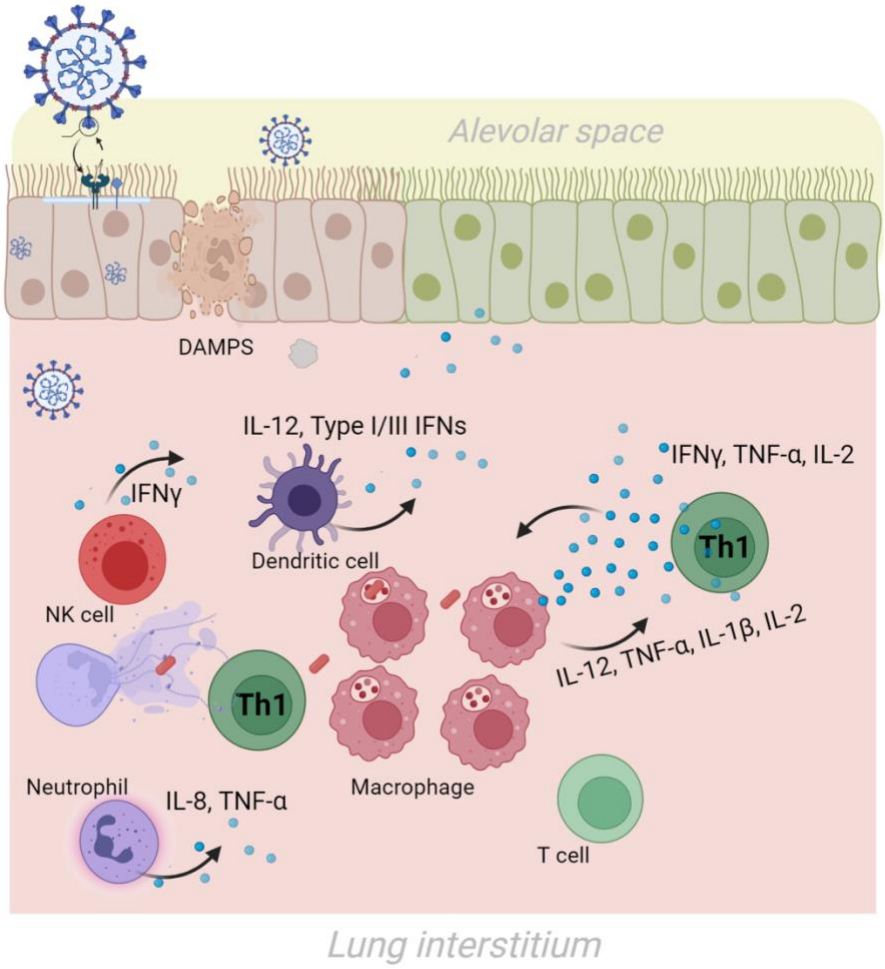

***Figure 1.5**. M.tb and SARS-CoV-2 co-infection. Prior infection with M.tb will likely lead to an active immune response characterized by recruitment of innate cells and Th1 cells, which produce various proinflammatory cytokines including TNF-α, IL-2, IL-12, IL-1β, and IFNγ. This active response will then be present in lung prior to SARS-CoV-2 co-infection, which will be entering a primed lung environment. Image created using Biorender.*

CHAPTER 2. M.TB DIMINISHES SARS-COV-2 SEVERITY THROUGH INNATE IMMUNE PRIMING

This chapter was reproduced from the following article:

Williams Brittany D. , Ferede Debora , Abdelaal Hazem F. M. , Berube Bryan J. , Podell Brendan K. , Larsen Sasha E. , Baldwin Susan L. , Coler Rhea N. Protective interplay: Mycobacterium tuberculosis diminishes SARS-CoV-2 severity through innate immune priming. *Frontiers in Immunology* 15 (2024). doi: 10.3389/fimmu.2024.1424374.

2.1 Abstract

At the beginning of the COVID-19 pandemic those with underlying chronic lung conditions, including TB, were hypothesized to be at higher risk of severe COVID-19 disease. However, there is inconclusive clinical and preclinical data to confirm the specific risk SARS-CoV-2 poses for the millions of individuals infected with M.tb. We and others have found that compared to singly infected mice, mice co-infected with M.tb and SARS-CoV-2 leads to reduced SARS-CoV-2 severity compared to mice infected with SARS-CoV-2 alone. Consequently, there is a large interest in identifying the molecular mechanisms responsible for the reduced SARS-CoV-2 infection severity observed in M.tb and SARS-CoV-2 co-infection. To address this, we conducted a comprehensive characterization of a co-infection model and performed mechanistic in vitro modeling to dynamically assess how the innate immune response induced by M.tb restricts viral replication. Our study has successfully identified several cytokines that induce the upregulation of anti-viral genes in lung epithelial cells, thereby providing protection prior to challenge with SARS-CoV-2. In conclusion, our study offers a comprehensive understanding of the key pathways induced by an existing bacterial infection that effectively restricts SARS-CoV-2 activity and identifies candidate therapeutic targets for SARS-CoV-2 infection.

2.2 Introduction

COVID-19, caused by infection with SARS-CoV-2, has resulted in a global pandemic that has claimed over 6.8 million lives as of March 2024 (43). Initially, individuals with underlying chronic lung conditions, including TB, were thought to be at higher risk of severe COVID-19 and ARDS (105). This was a great concern for the 10 million individuals diagnosed with TB in 2019 (1). To speak to its detriment, TB was the long-standing number one infectious disease killer until the start of the COVID-19 pandemic (1). Although the prevalence of COVID-19 and TB co-infection has not been officially confirmed, a recent meta-analysis of 18 studies estimated that the prevalence of TB among COVID-19 positive patients was 1.1% in America, 1.5% in Asia and 3.6% in Africa (106). While TB was later removed as a significant risk factor, conclusive data on

the specific risk SARS-CoV-2 poses for the millions infected with M.tb remains elusive. Early clinical reports presented conflicting findings with some noting that TB was not a major determinant of mortality (84, 105, 107) and others suggesting co-infection led to worsened outcomes of COVID-19 (81, 108).

Additionally, a longitudinal global cohort study which found survival was lower among co-infected individuals discovered certain risk factors, such as age, HIV co-infection, male sex, and invasive ventilation, influenced adverse TB and COVID-19 outcomes (109). Therefore, highlighting multiple factors that may contribute to an individual's response to SARS-CoV-2 and M.tb infection. While the characterization of the immune response within co-infected individuals has also been limited, studies have reported both overlapping and distinct immune responses (110-112). A clinical study characterizing plasma immune profiles of individuals with TB and COVID-19 versus singular TB or COVID-19 discovered an immune signature composed of TNF-α, MIP-1β, and IL-9 that discriminated co-infection from COVID-19 alone (111). In addition, a signature of TNF-α, IL-1β, IL-17A, IL-5, fibroblast growth factor-basic, and granulocyte macrophage colony stimulating factor (GM-CSF), has discerned co-infected individuals from those with TB only (111). Indeed, there seems to be a nuanced relationship between M.tb infection and SARS-CoV-2 and multiple demographic and clinical factors may alter the immune response to both infections (105).

Understanding how these two pulmonary pathogens interact starts with examining their individual induced innate immune responses, as these responses represent the first line of defense against pathogens. Primary infection of angiotensin converting enzyme-2 (ACE2)-expressing airway and alveolar epithelial cells by SARS-CoV-2 initiates viral replication, pyroptosis of host cells, and activation of innate immune pathways (113). The innate immune response when properly activated is crucial in providing protection against early SARS-CoV-2 infection. Several pattern recognition receptors (PRRs) detect SARS-CoV-2 and initiate innate responses, including endosomal toll-like receptor 3 (TLR3) and toll-like receptor 7 (TLR7)

signaling pathways, as well as cytoplasmic RNA sensor, melanoma differentiation-associated protein 5 (MDA5) (72, 114, 115). The cytoplasmic RNA sensor, retinoic acid-inducible gene I (RIGI), acts more as a restriction factor in which RIG-I detection of the SARS-CoV-2 genome hinders the virus's first step of replication. Furthermore, knock out of RIG-I was shown to enhance viral activity and virus restriction was rescued with upregulation of RIG-I expression (116). Upon activation of the PRRs, downstream signaling results in the production of antiviral IFNs, and cytokines and chemokines which create an anti-viral environment and recruits innate cells to the site of infection (117).

Type I, II, and III IFNs have been heavily focused on due to their ability to inhibit SARS-CoV-2 replication (118-122). IFN antiviral activity is driven by the upregulation of ISGs, which have multiple mechanisms in restricting viral activity (103, 123, 124). Multiple ISGs which broadly act against SARS-CoV-2 by inhibiting viral entry, viral RNA synthesis, and virion assembly, have also been identified (124). However, SARS-CoV-2 has evolved multiple strategies to evade initial innate immune responses, including blocking recognition by host sensors such as RIG-I, MDA5, and TLRs and inhibiting IFN signaling, thus promoting viral replication (75, 125, 126). This immune evasion is thought to delay immune responses, leading to unchecked viral replication, high viral load, and a subsequent dysregulated immune response. The resulting disproportionate response to SARS-CoV-2 infection is characterized by a robust release of proinflammatory cytokines and dysfunctional myeloid responses, including elevated levels of IL-2, IL-6, IL-7, IL-10, IL-12, and IL-1β, TNF-α, MCP-1α, IP-10, lymphopenia, and high lung infiltration of monocytes and T cells (113, 127-129).

In contrast to the acute hyperinflammatory profile associated with SARS-CoV-2, chronic M.tb infection is known to elicit a diverse array of proinflammatory and regulatory responses (130). Following initial infection, alveolar macrophages engulf M.tb bacilli, migrate to the lung parenchyma, and orchestrate the recruitment of various innate immune cells and effector T cells. While some infections resolve, others go on to result in granuloma formation, an attempt at

prolonged containment by the host and persistent but quiescent latent infection (131-134). Major cell types involved in the control of M.tb are pro-inflammatory T helper 1 (Th1) and Th17 CD4+ T cells which are largely recruited to form a lymphocytic cuff around a core granuloma structure containing macrophages and bacteria. Th1 and Th17 CD4+ T cells express IL-2, IFN-γ, and TNFα, or IL-17A, IL-21, and IL-23, respectively, which play critical roles in driving immune activation and inflammatory responses designed to control M.tb (34, 130). However certain hallmark stages of granuloma formation and persistent infection include the expression of anti-inflammatory cytokines IL-10, IL-27 and TGFβ to regulate T cell pro-inflammatory activity (34, 130). This balance of immune responses enables local containment of M.tb bacilli without more systemic inflammatory damage.

As previously discussed, further insights can be gleaned from other bacterial and viral co-infection studies. For instance, administering BCG, intravenously, but not subcutaneously, significantly protected mice from SARS-CoV-2 challenge, characterized by reduced lung inflammation and viral burden (93). Similarly, aerosolized exposure to nontypeable Haemophilus influenzae (NTHi) bacterial lysate before influenza A infection conferred protection, as evidenced by heightened inflammatory cytokines, decreased viral loads, and increased survival rates in treated mice (135). Notably, while both bacterial exposures provided protection against secondary viral infections, they triggered distinct immune responses, likely influenced by the route of administration, bacterial species and specific PRR pathways induced. These findings collectively underscore the role of nonspecific immune responses in defending against subsequent heterologous infections (136).

Given the global impact of the pandemic, delay of vaccine deployment in many TB endemic low- and middle-income countries (LMICs), and continuous emergence of hyper transmissible variants, it is unknown how long the pandemic and its ramifications will last. This highlights the need to study coinfections to identify disease burdens, mechanisms of

immunopathology, and heterologous protection to better inform susceptibility and population risk. With our work, we tested our hypothesis that acute M.tb infection induces a diffuse innate immune response within the lungs leading to a primed lung epithelium that limits viral replication, provides non-specific protection against SARS-CoV-2-induced lung viral burden, and host morbidity in a co-infection mouse model. In this study, by characterizing a discrete co-infection model using virulent M.tb and variant of high importance and incorporating in vitro studies we aimed to uncover the mechanism that could be leading to the observed protection.

2.3 Results

2.3.1 Active M.tb infection enhanced host survival and decreased viral burden after SARS-CoV-2 challenge

We hypothesized that infecting mice first with M.tb to induce an active infection and subsequent immune response, followed by co-infection with SARS-CoV-2, could potentially alter disease outcomes and affect survival endpoints. Highly virulent W-Beijing clinical strain, M.tb HN878, was delivered as a low dose aerosol challenge (LDA, 50–100 bacteria) to female and male K18-hACE2 mice. Three weeks post-M.tb infection, mice were challenged with 200 plaque forming units (PFU) of SARS-CoV-2 Beta. (**Figure 2.1A**). Male and Female mouse cohorts (n=10 per sex) were assessed for survival following infection with M.tb, SARS-CoV-2, or co-infection. Mice singularly infected with SARS-CoV-2 had significantly lower survival rates compared to those in the saline or M.tb infected groups. However, the M.tb and SARS-CoV-2 co-infected group showed a significantly higher survival rate than the group infected solely with SARS-CoV-2 (**Figure 2.1B**). The increased survival amongst the co-infection group versus the singular SARS-CoV-2 infection group suggests prior M.tb infection may provide partial protection from SARS-CoV-2 challenge, in alignment with our hypothesis.

Viral titers of SARS-CoV-2 were evaluated locally and systemically to determine if co-infected mice have differences in viral load magnitude or distribution. In alignment with prior work (137-139), the co-infected group exhibited decreased lung viral titers at day 1 post-co-infection

and significantly decreased lung and lymph node viral titers at day 3 post-co-infection, the anticipated viral peak of our collection timeline, compared to SARS-CoV-2 alone cohorts (**Figure 2.1C**). There was no difference in viral burden in brain samples when comparing the two infection groups (**Figure 2.1C**). There was no difference in CFU between the groups for all organs and time points, suggesting the exhibited protection from morbidity was not due to a change in M.tb burden (**Figure 2.1D**).

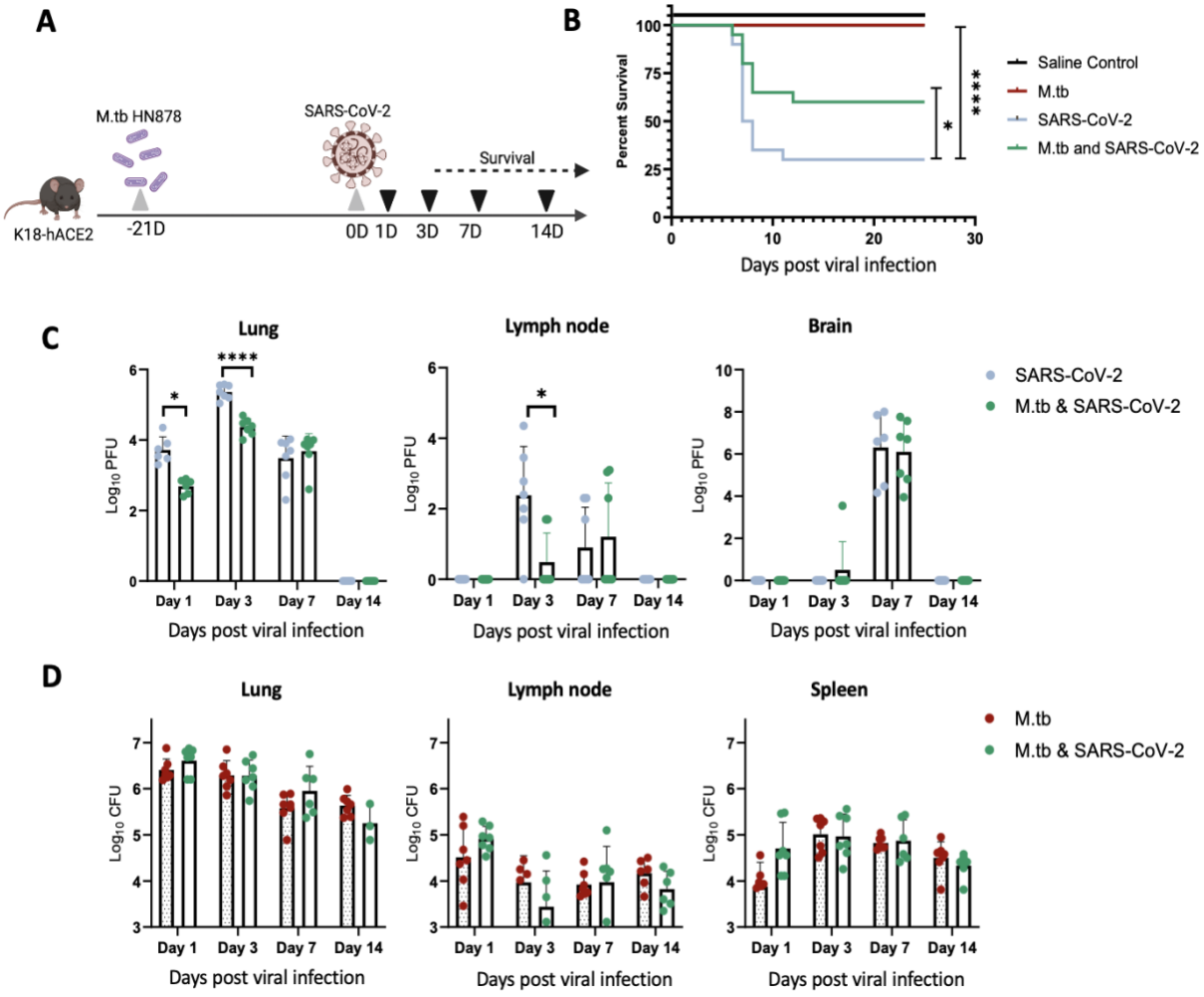

Figure 2.1. M.tb and SARS-CoV-2 co-infection animal model. (A) Experiment scheme for M.tb and SARS-CoV-2 co-infections including selected analysis time points. Image made with Biorender. (B) Survival analysis of male and female infection groups with 20 mice per group (10 mice per sex). Mouse weights (n=20/group) were recorded daily, and percent weight change calculated from the maximum recorded weight. (= P<0.05, Mantel-Cox and Wilcoxon). (C) Lung, lymph node and brain homogenates from seven female mice per group were used in a plaque formation assay (PFA) to measure viral titers. Each time point analyzed using unpaired T-Test with Welch's T Test and alpha of 0.05 (* = P<0.05, **= P<0.01, ***=P<0.001, ****= P<0.0001). (D) Lungs, lymph node and spleen homogenates from seven female mice per group were plated on 7H10 agar triplates to measure bacterial burden. Figure 2.1 was reproduced from* (140) with permission*, Creative Commons Attribution 4.0 International License*.

We have previously seen that bacterial burden can be uncoupled from pulmonary pathology in mouse models of TB, where pulmonary disease and morbidity endpoints may be driven more by host factors (141). Interestingly, when assessing the lung pathology in these co-infection studies (**Figure 2.2A**) there was no significant difference in percent lesion area between co-infected animals and the SARS-CoV-2-only infected group at day 1 (**Figure 2.2B**). However, by day 7 there was a trend towards decreased lesion scores in the co-infected groups compared to the M.tb only infection group (**Figure 2.2D**), which became significant by day 14 (**Figure 2.2E**). This trend has been published previously (138) and speaks to the complexities of lung pathology in the context of co-infection. Conducting additional analysis which more clearly defines the differences between TB and COVID-19 pathology is worth further exploration. While these data suggest infection with SARS-CoV-2 may help resolve acute lesions from existing M.tb infection

(**Figure 2.2E**), the primary focus of this work is to determine how infection with M.tb establishes an inhospitable pulmonary environment for SARS-CoV-2.

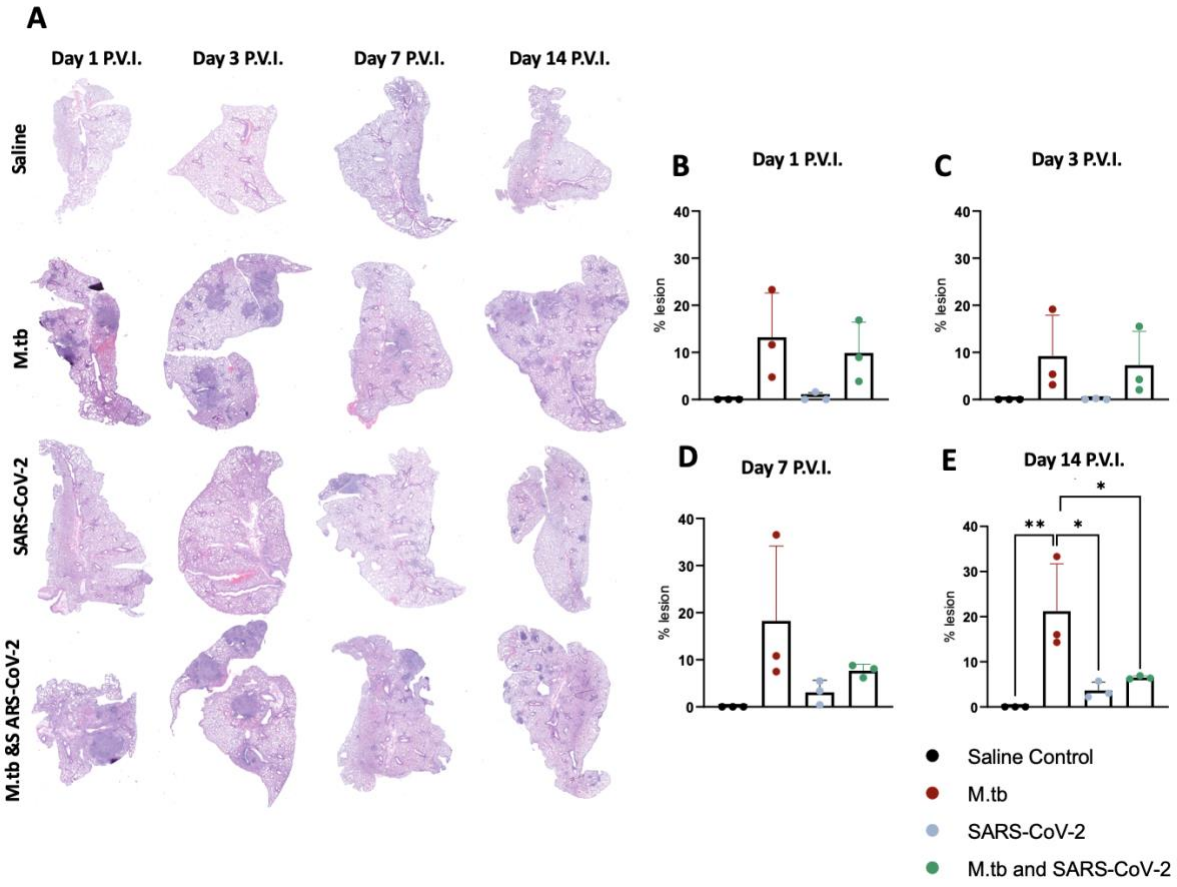

Figure 2.2. *Kinetic quantitative lung histopathology among infection groups. (A) Representative H&E images of accessory lung lobe sections showing the presence of pulmonary lesions (dark purple). (B) Percent lesion was calculated by dividing the lesion area by the non-lesion area. Each time point was analyzed using one-way ANOVA alpha of 0.05 (* = P<0.05, **= P<0.01). Figure 2.2 was reproduced from* (140) *with permission, Creative Commons Attribution 4.0 International License*.

2.3.2 Established M.tb infection influences lung inflammation during acute SARS-CoV-2 infection

Given the partial protective phenotype displayed by the co-infection model, the immune profiles of M.tb-infected, SARS-CoV-2-infected and co-infected animals were evaluated. Using flow cytometry, the kinetic influx of immune cells to the lung following co-infection were compared to the other cohorts. Both M.tb-infected mice (21 days post infection) and M.tb-infected mice subsequently infected with SARS-CoV-2 (co-infected group) showed elevated

levels of neutrophils and macrophages at the day 1 and 3 post-virus challenge time points, and increased influx of T cells and NK cells at day 3 compared to the group infected with SARS-CoV-2 only (**Figure 2.3**). Absolute cell counts mirroring these trends were also observed (Appendix supplementary figure A.2).

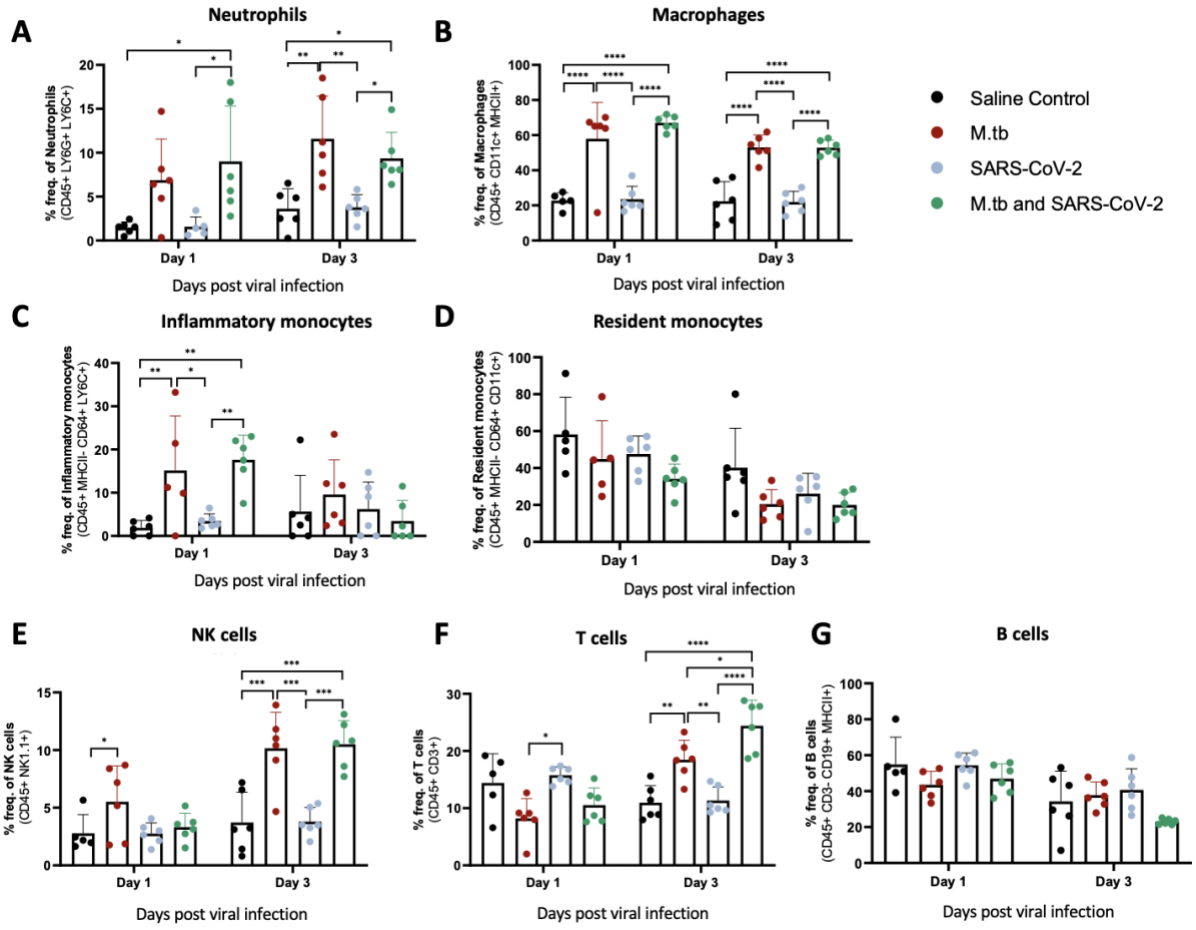

Figure 2.3. *Measured cell populations in mouse lungs following singular infection with M.tb and SARS-CoV-2, and co-infection over time. (A-G) Whole lungs from six mice per group per time point were homogenized, processed, and stained for surface markers to measure percent frequency of immune cell populations at 1 day or 3 days following SARS-CoV-2 infection. Significant differences between cohorts at each time point were determined by One-way ANOVA, alpha of 0.05 (* = P<0.05, **= P<0.01, ***=P<0.001, ****=P<0.0001). Figure 2.3 was reproduced from* (140) *with permission, Creative Commons Attribution 4.0 International License*.

This showcases the influence chronic M.tb infection has on the inflammatory environment of the lung. Bronchioalveolar lavage fluid (BALF) from M.tb-infected and co-infected mice contained significantly elevated IL-6, TNF-α, IFNγ, IP-10, MIP-1a, MCP-1, and KC-GRO at days 1 and 3 post-co-infection, while the SARS-CoV-2 infection group displayed delayed induction of these

same effector molecules until day 7 (**Figure 2.4**). Interestingly, there was an absence of strong kinetic patterns of increases or persistent decreases in inflammatory gene expression within the lung across infection groups (**Figure 2.5A-C**). On day 3 there were trends of increased expression in certain ISGs, PRRs and inflammatory pathway genes in M.tb and co-infected groups (**Figure 5B** and appendix supplementary Figure A.4).

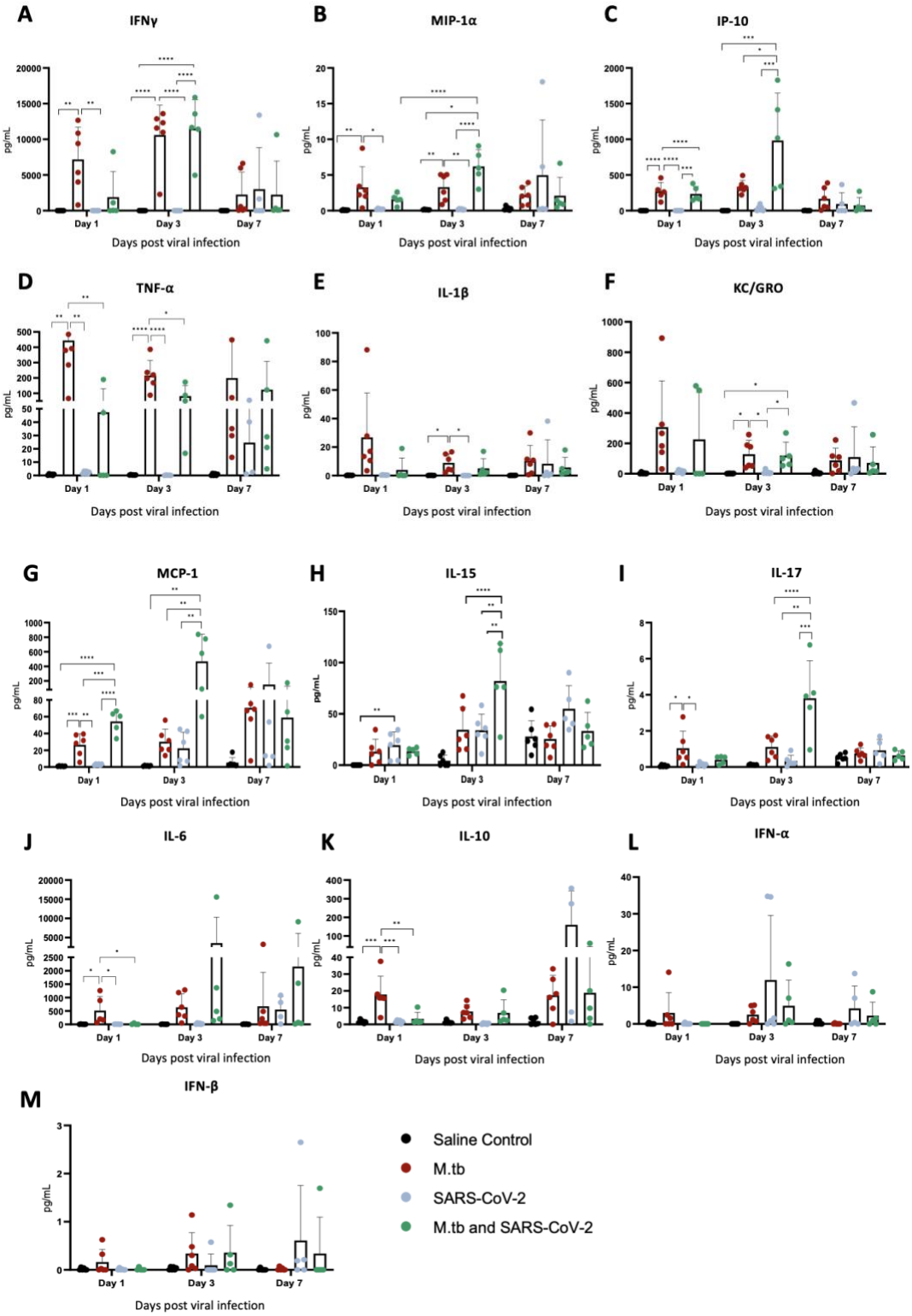

Figure 2.4. *Cytokine and chemokine responses in the lung early after infection with SARS-CoV-2 or co-infection with M.tb. (A-M) Bronchoalveolar lavage fluid from seven female mice per group was collected 1, 3, and 7-days post-infection with SARS-CoV-2. Significant differences between cohorts at each time point was determined by one-way*

ANOVA, alpha of 0.05 (= P<0.05, **= P<0.01, ***=P<0.001, ****=P<0.0001). Figure 2.4 was reproduced from* (140) *with permission, Creative Commons Attribution 4.0 International License*.

The increased inflammatory response observed in the co-infected group was initially surprising since the robust pro-inflammatory response has been identified to be detrimental in SARS-CoV-2 infection (113). However, the timing and type of immune response induced may be important for priming the lung to combat SARS-CoV-2 infection. Mechanistic in vitro studies were next used to evaluate which innate immune response induced by the primary M.tb infection provide protection against subsequent SARS-CoV-2 infection.

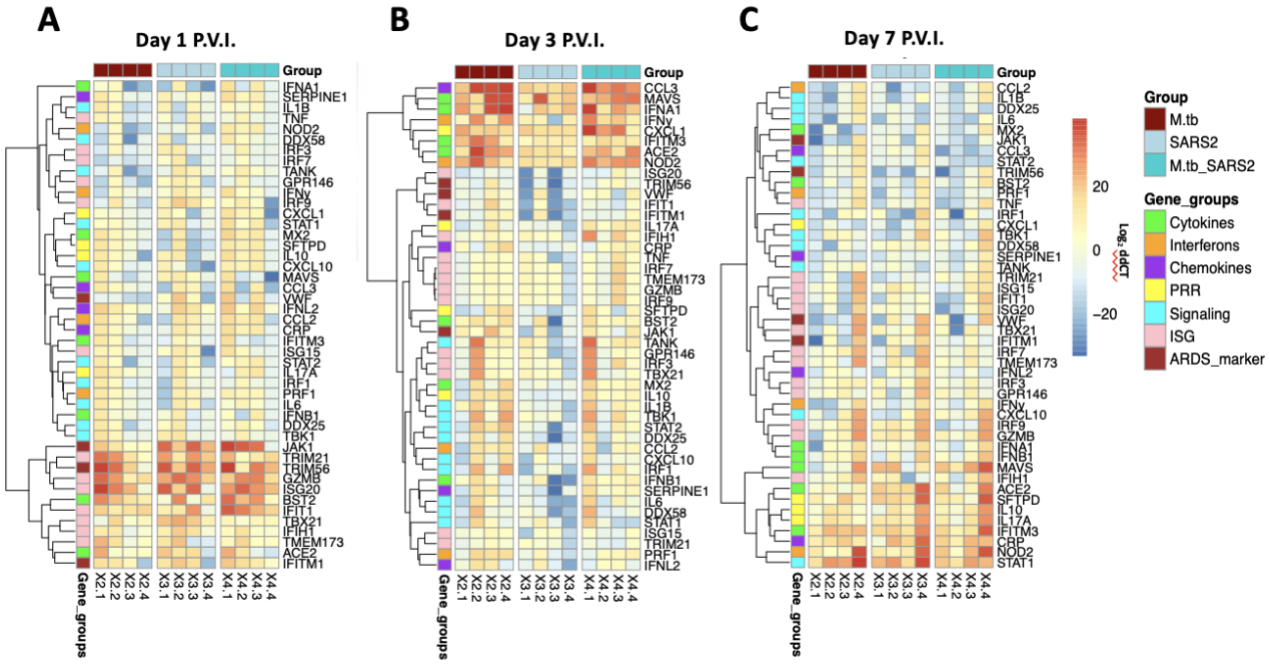

Figure 2.5. *Lung mRNA expression of inflammatory-related genes early after infection with SARS-CoV-2 or co-infection with M.tb. Accessories lobes from four female mice per group were collected 1, 3, and 7-days post-SARS-CoV-2 infection used in RT-qPCR to measure the delta-delta CT values. Heat map depicts Log2 relative expression (delta-delta CT) of selected cytokines, chemokines, IFNs, ISGs, and genes involved in inflammatory pathways and lung inflammation (A) 1-day post SARS-CoV-2 infection (B) 3-days post SARS-CoV-2 infection, and (C) 7-days post SARS-CoV-2 infection. Expression was normalized to non-infected saline control mice. Graphs were created using RStudio.* ***Figure 2.5*** *was reproduced from* (140) *with permission, Creative Commons Attribution 4.0 International License*.

2.3.3 Cytokines produced from M.tb infected PBMCs provide passive protection from SARS-CoV-2 challenge in vitro

To model co-infection in vitro, PBMCs were infected with M.tb, as they serve as niche host cells and are responsive to infection. Conversely, SARS-CoV-2 infection was modeled using permissive epithelial cells, which fulfill a similar role. While lung epithelial cells show limited direct responsiveness to M.tb, they exhibit heightened reactivity and transcriptional changes when exposed to M.tb-infected myeloid cells (142). Our investigation aimed to determine whether cytokines generated during initial M.tb infection of immune cells could confer protection against secondary SARS-CoV-2 infection in susceptible bystander epithelial cells.

We used PBMCs from healthy male and female donors, collected before and after 2019, as well as from BCG-immunized donors (Appendix supplementary data A.5), to investigate the effects of prior SARS-CoV-2 exposure or BCG immunization on immune responses. There was additional interest in investigating prior BCG immunizations given the attenuated M. bovis vaccine is currently the only licensed TB vaccine and regularly administered in TB endemic regions. While early in the pandemic there were hypotheses that prior BCG immunization may provide protection against SARS-CoV-2 (143), these claims were later dispelled in clinical studies (92, 144). Frozen PBMCs were thawed and either mock-infected or infected with M.tb HN878 at a MOI of 1 for 96 hours (**Figure 2.6A**). Supernatants were harvested, filtered, and applied to Vero cells, which are highly permissive to SARS-CoV-2 infection, to assess whether cytokines alone could confer protection against SARS-CoV-2 infection. Treatment of Vero cells with supernatants from M.tb-infected PBMCs resulted in significantly reduced viral titers, with no significant differences observed among PBMC groups defined by date or vaccination history (**Figure 2.6B**). These findings were confirmed using more physiologically relevant Calu-3 human airway epithelial cells (145-147) where diminished viral titers were observed in samples pre-treated with supernatants from M.tb-infected PBMCs (**Figure 2.6C**). To define the essential elements of protection, the cytokine levels within the supernatants were quantified, revealing increased production of several proinflammatory cytokines, including G-CSF, GM-CSF, TNF-α, IL-1β, IL-6, and IFNγ, following M.tb infection compared to mock-infected PBMCs (**Figure 2.6D**). Given the absence of significant

differences between PBMC groups, subsequent experiments were conducted using PBMCs collected prior to 2019…

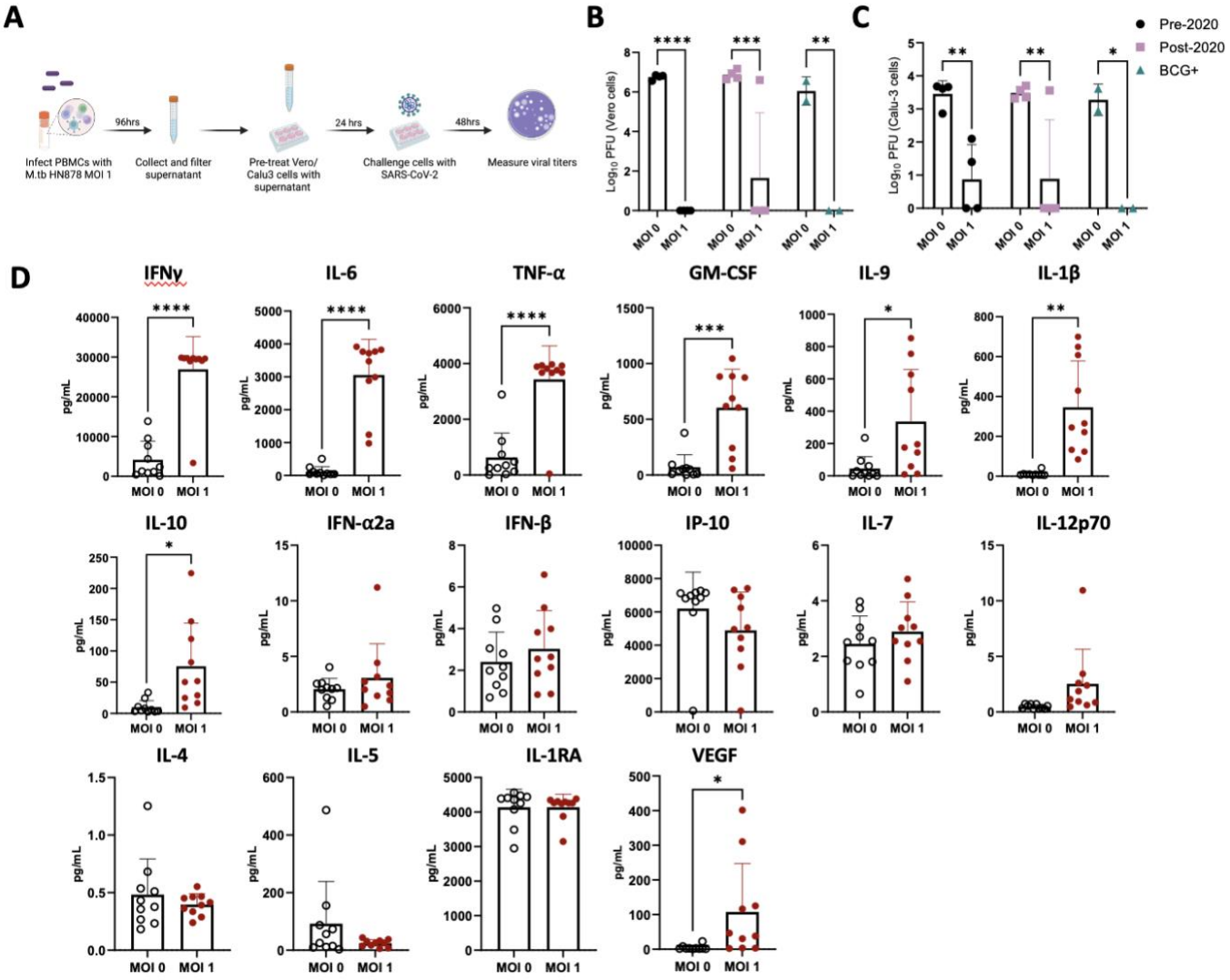

Figure 2.6. *Cytokine levels from M.tb-infected PBMCs and the effect of M.tb infected PBMC supernatants on viral replication in cell culture. (A) Experimental scheme of in vitro PBMC M.tb infection. (B) Viral titers of SARS-CoV-2-challenged Vero cells treated with supernatants from mock-infected or M.tb-infected human PBMCs collected prior to 2020 (N=4), post-2020 (N=4), or from BCG-immunized patients (N=2), and (C) viral titers of SARS-CoV-2-challenged Calu-3 cells treated with supernatants from mock-infected or M.tb-infected human PBMCs collected prior to 2020 (N=4), post-2020 (N=4), or from BCG-immunized patients (N=2). Titers between mock-infected and M.tb-infected supernatant treatments for each PBMC group were analyzed using two-way ANOVA (* = P<0.05, **= P<0.01, ***=P<0.001, ****= P<0.0001). (D) Cytokine measurements of supernatants from mock-infected or PBMCs infected with M.tb HN878 at a MOI of 1. Measurements analyzed using unpaired T-Test with Welch's T Test and alpha of 0.05 (* = P<0.05, **= P<0.01, ***=P<0.001, ****= P<0.0001). Figure 2.6 was reproduced from (137) with permission, Creative Commons Attribution 4.0 International License.*

Supernatant-treated Calu-3 cells were then used in RT-qPCR analysis to determine if cells underwent transcriptional changes upon treatment with supernatants. Treated Calu-3 cells

showed significantly increased expression of ISGs such as OAS1, OAS3, MX2 and notably, IFIH1, the gene encoding MDA5, a primary PRR for SARS-CoV-2, compared to media-treated cells (**Figure 2.7A**). Subsequently, 24 hours post-SARS-CoV-2 infection, the expression of these ISGs increased in both control and M.tb-infected PBMC supernatant-treated cells, with a significant increase in expression sustained in the supernatant-treated cells (**Figure 2.7B**). These findings support our hypothesis that prior M.tb infection primes epithelial cells towards resisting viral infection by inducing ISG expression.

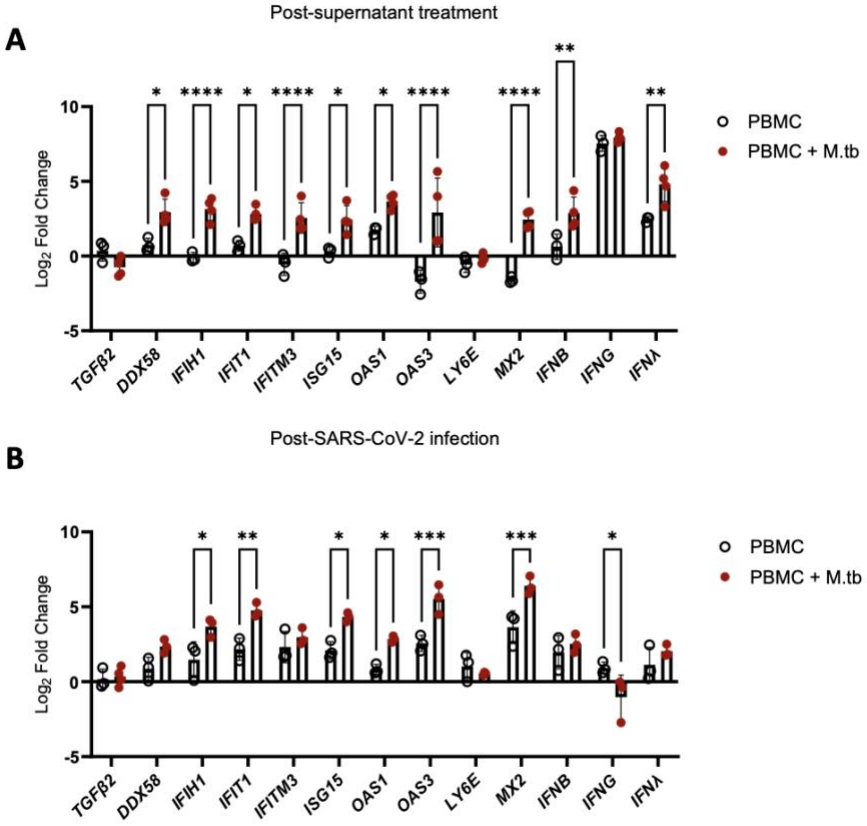

Figure 2.7*. Gene expression changes in Calu-3 epithelial cells treated with supernatants from mock-infected or M.tb-infected human PBMCs and infected with SARS-CoV-2. Graphs depict fold-change expression of ISGs normalized to media-treated cells and the Beta-Actin house-keeping gene. (A) upregulation of genes 24 hours post-supernatant treatment and (B) upregulation of genes 24 hours post-SARS-CoV-2 infection. Expression of genes between mock-infected and M.tb-infected supernatant treatments was analyzed using two-way ANOVA (* = P<0.05, **= P<0.01, ***=P<0.001, ****=P<0.0001). Figure 2.7 was reproduced from (137) with permission, Creative Commons Attribution 4.0 International License.*

2.3.4 Passive protection from prior M.tb infection restricts viral replication

While pre-treatment led to transcriptional changes and protection from SARS-CoV-2 after 48 hours of infection, pinpointing the stage of the viral infection cycle that may be affected was of interest. To align with our transcriptional data, Calu-3 cells were treated with supernatants or media (positive control) and infected with SARS-CoV-2 for 1, 6, 24, and 48 hours, then assessed for viral load. Following 1 hour of infection, no significant differences in viral load were observed (**Figure 2.8A**), suggesting no influence or perturbations in viral entry pathways—a result consistent with the expected SARS-CoV-2 doubling time of around 6 hours (148). However, after 6 hours of infection, there was a noticeable trend toward decreased titers in treated Calu-3 cells (**Figure 2.8B**). By 24 hours, treated cells displayed no plaques likely reaching the limit of detection (**Figure 2.8C**), suggesting that treated cells were not permissive to replication and actively eliminated the virus, thereby conferring protection.

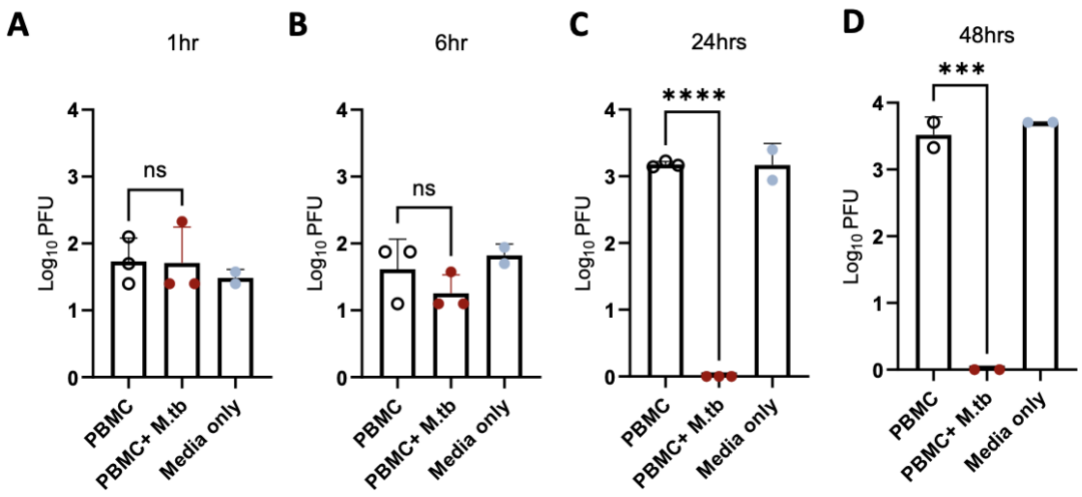

Figure 2.8*. Viral load in Calu-3 cells treated with supernatants from mock-infected or M.tb-infected human PBMCs following infection with SARS-CoV-2. Calu-3 cells were treated with supernatants and infected with 75 PFU of SARS-CoV-2 for (A) 1 hour, (B) 6 hours, (C) 24 hours, and (D) 48 hours. Significant differences between groups at each time point was determined by one-way ANOVA, alpha of 0.05 (* = P<0.05, **= P<0.01, ***=P<0.001, ****=P<0.0001). Figure 2.8 was reproduced from (137) with permission, Creative Commons Attribution 4.0 International License.*

2.3.5 Neutralization of IFNγ attenuates protection against SARS-CoV-2

To explore the mechanism of protection, an investigation into the involvement of specific cell types and cytokines was conducted. While type I IFNs are normally associated as the

predominant anti-viral response, we did not see significant levels within our measurements. However, we did detect significant levels of IFNγ in both in vivo and in vitro models, and wanted to determine if blocking IFNγ would attenuate the observed protection. Accordingly, major cell types known to induce IFNγ were targeted.

Human PBMCs were co-incubated with neutralizing antibodies against CD4+ T cells, CD8α+ T cells, CD314+ NK cells, and IFNγ at increasing concentrations, and then infected with M.tb for 96 hours. Mouse IgG1 and IgG2 antibodies were used as isotype negative controls, while media-only treated cells served as a control for viral replication. After the 96-hour incubation period, supernatants were collected, as previously described, and used to treat permissive Vero cells to measure PFU following SARS-CoV-2 infection. Blocking of CD314+ NK cells did not result in a significant increase in viral titer, and CD8α+ T cells reached significance only at the highest concentration (**Figure 2.9**). Neutralization of IFNγ led to diminished protection at 20 and 100 μg/mL, as evidenced by an increase in viral titer, highlighting its importance in conferring protection against SARS-CoV-2 (**Figure 2.9**).

Interestingly, neutralization of CD4+ T cells resulted in an increased viral load with escalating antibody concentrations, suggesting that protection could be dependent on IFNγ and CD4+ T cell activity.

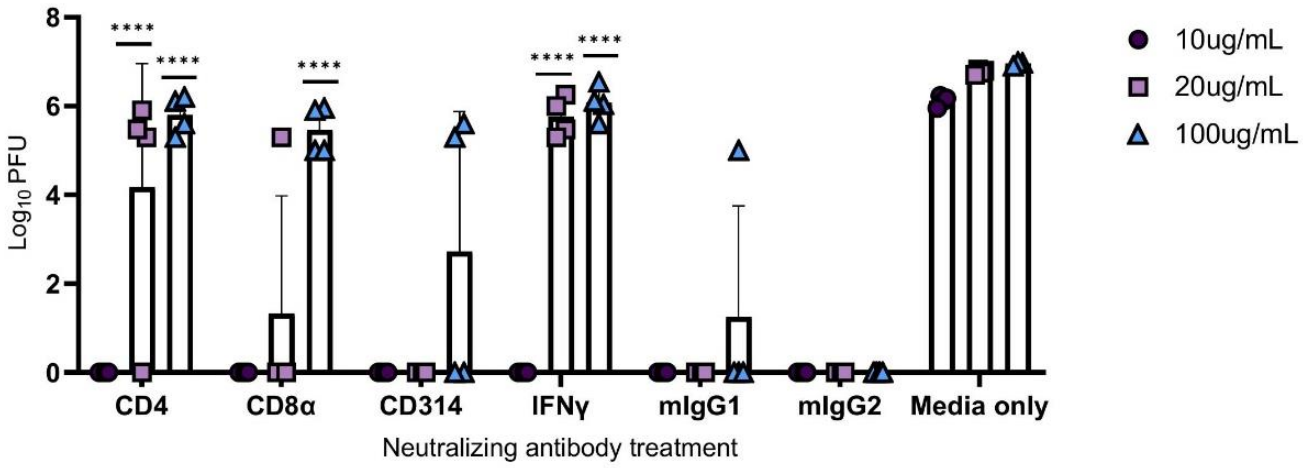

Figure 2.9*. Viral titers following the administration of neutralizing antibodies against immune components. PBMCs were infected with M.tb in the presence of neutralizing antibodies against CD4, CD8α, CD314, and with isotype controls mouse IgG1 (mIgG1) and IgG2 (mIgG2). Some collected supernatants were treated with neutralizing antibodies against IFNγ. Vero cells were treated with the supernatants then challenged with SARS-CoV-2 and PFU recorded 48 hours post-infection. Significant differences of PFUs between neutralization treatments and relative isotype controls, mouse IgG1 (CD4, CD314, and IFNγ) and IgG2 (CD8α) were analyzed using two-way ANOVA (****=P<0.0001). Data are representative of two independent experiments. Figure 2.9 was reproduced from (137) with permission, Creative Commons Attribution 4.0 International License.*

2.4 Discussion

TB and COVID-19 remain leading infectious disease killers, with 1.3 million TB-related deaths reported by the WHO in 2022 (2) and a cumulative 6.8 million COVID-19-related deaths as of March 2024 (43). The lack of definitive clinical data on the risks associated with M.tb and SARS-CoV-2 co-infection has sparked significant interest in understanding the interplay between these pathogens. In this study, we contribute to the growing body of data on co-infection using a preclinical model, which allows for the investigation of specific interactions between infections while controlling for factors that influence disease outcomes. This is crucial given the challenges observed in many clinical studies on M.tb and SARS-CoV-2 co-infections, such as issues with study sizes, comorbidities, coinciding risk factors and unknown infection timelines. Consistent with previous findings, we observed a protective effect against SARS-CoV-2 following prior M.tb infection. This model is additive and unique given variations in pathogen strains, including clinical

M.tb isolates and variants of interest. By pairing in vivo results with in vitro mechanistic studies, we were able to specifically examine the impact of M.tb-induced immune responses on epithelial cells, which are the primary targets of SARS-CoV-2. This focused approach addresses potential limitations of complex in vivo systems.

From our studies, we elucidated the importance of IFNγ and CD4+T cell activity in driving the protection seen in vitro. An early, and Th1-leaning CD4+ T cell response is deemed important for combatting SARS-CoV-2 (149). Additionally, a study has shown that pre-existing CD4+ T cells induced from previous infection provided protection against SARS-CoV-2 (150). Similarly, IFNγ has demonstrated driving vaccine-induced cellular immunity in K18-hACE2 transgenic B-cell deficient (μMT) mice (151) and recently confirmed to induce early control of SARS-CoV-2 infection when administered intranasally to wildtype C57BL/6 mice (152). Interestingly, clinical studies have reported on M.tb and SARS-CoV-2 co-infected individuals' limited cellular response to M.tb or SARS-CoV-2 antigens potentially due to anergy or immune exhaustion (110, 153, 154). However, we hypothesize that while prior M.tb induced immune priming can be protective during acute SARS-CoV-2 infection, in certain individuals other factors may hinder this protection, allowing for co-infection to persist and worsening disease outcomes. While we were able to get a controlled look at M.tb and SARS-CoV-2 co-infection in a preclinical model there are many other conditions to consider that may affect co-infection in clinical contexts.

In turn, we remain curious about how our use of a low-dose M.tb infection model, which more closely mimics the chronic stage of human infection, may contribute to the observed protection. Exploring the ultra-low dose M.tb model (155), which delivers 1-3 CFU and strongly mirrors human pathology, may provide insight into whether the diffuse lung immune response exhibited with a low-dose model, or other factors drive protection in co-infection models. Interestingly, it has been reported that the magnitude of viral titers inversely correlated with increasing M.tb infectious dose (126), providing further evidence towards the need of a diffuse infection and accompanied response. Additionally, LMICs with large TB burden are heavily

associated with comorbidities that affect TB and COVID-19 severity (156-158). To further understand and close the gap between preclinical and clinical studies investigating these additional factors such as sex, metabolic diseases, age, HIV co-infections, and antibiotic resistant M.tb strains in the pre-clinical model, will be vital for furthering knowledge on M.tb and SARS-COV-2 co-infections. Additionally, we acknowledge that differences based on the phase of M.tb infection, such as active versus latent infection, can impact the outcomes of co-infection with SARS-CoV-2, thus warranting further investigation.

Moreover, our study underscores the importance of innate immune induction in protection against SARS-CoV-2. While increased global vaccination has significantly impacted the trajectory and harm of COVID-19, the emergence of humoral immune evasion by SARS-CoV-2 variants of concern highlighted the need for more comprehensive vaccine-induced responses. Our findings further emphasize the crucial role of innate immune responses in combating the earliest stages of viral infections. Additionally, this highlights the need to fine-tune inflammatory responses to ensure they contribute to protection rather than exacerbate detrimental effects. These models help winnow down potential therapeutic targets and define features desirable for prophylactic vaccine strategies.

2.5 Methods

2.5.1 Preclinical mouse model

Female and Male K18-hACE2 mice [strain: 2B6.Cg-Tg(K18-ACE2)2Prlmn/J], 6-8 weeks of age were purchased from Jackson Laboratory (Bar Harbor, ME). Mice were housed under pathogen-free conditions at Seattle Children's Research Institute (SCRI) biosafety level 3 animal facility and were handled in accordance with the specific guidelines of SCRI's Institutional Animal Care and Use Committee (IACUC). Mice were infected with a low dose (50-100 bacteria) aerosol (LDA) of M.tb HN878 using a Glas-Col whole-body exposure chamber (Glas-Col, Terre Haute, IN). Twenty-four hours post challenge the lungs of three mice were homogenized and plated on Mitchison 7H11 agar (Thermo Fisher Scientific, Waltham, MA) to confirm delivery of 50-100 CFU

per mouse. For SARS-CoV-2 infection mice were first put under anesthesia with intraperitoneal (i.p.) administration of Ketamine (Patterson Veterinary, Loveland, CO) and Xylazine (Patterson Veterinary). SARS-CoV-2 clinical isolates were administered at 200 PFU via intranasal installation of 40µL per nare. Following SARS-CoV-2 infection mice were weighed daily. Animals that reached 20% weight loss and/or exhibited physical signs of morbidity were humanely euthanized.

2.5.2 Cells and pathogens

Vero TMPRSS2 (National Institute for Biological Standards and Control (NIBSC), Hertfordshire, England), Vero E6 (ATCC, Manassas, VA), and Calu-3 epithelial cells (ATCC) were maintained at 37 °C + 5% CO2 in Dulbecco's modified Eagle's medium (DMEM) supplemented with 10% fetal bovine serum (FBS), 2 mM L-glutamine, and 1% penicillin/streptomycin (cDMEM). Cells were tested regularly for mycoplasma with Mycoplasma PCR detection kit (MilliporeSigma, Burlington, MA).

SARS-CoV-2 Beta (hCoV-19/SouthAfrica/KRISP-EC-K005321/2020) was obtained from BEI Resources and housed under standard BSL-3 laboratory conditions. SARS-CoV-2 virus was propagated and titered by plaque assay in Vero E6 cells. Cultured cells were infected with the original stock at a MOI of 0.1 and incubated at 37 °C + 5% CO2 for 72 h. Supernatants were harvested, centrifuged to remove debris, aliquoted and frozen at −80°C.

2.5.3 Bacterial counts

At the indicated time points harvested organs were homogenized in DMEM using gentleMACS Octo Tissue Dissociator (Miltenyi, Bergisch Gladbach, Germany). Serial dilutions of organ homogenates were made in PBS with 0.05% Tween80, and aliquots of dilutions were plated on Middlebrook 7H10 agar tri-plates (Molecular Toxicology, Boone, NC), as previously described (141, 159). After 3-4 weeks of incubation at 37°C + 5% CO2, colony counts were recorded. Bacterial burden, in colony forming units (CFU) per organ, was calculated, and expressed as Log10.

2.5.4 Viral load measurements

Viral burden was measured with the plaque forming assay (PFA) using similar techniques described previously (160). Vero TMPRSS2 cells were plated in 6-well plates one day prior to titers at 4.8x105 cells/mL in 2mL of cDMEM per well. Harvested organs were homogenized in DMEM containing 1% FBS (D1 media) using the gentleMACs Octo Dissociator. Organ homogenates were serially diluted ten-fold using D1 media and added dropwise to the plated Vero cells. Plates were incubated at 37 ˚C + 5% CO2 for 60 minutes, with 15-minute intervals of rocking plates in all directions. After 60 minutes, 2mL of overlay media comprised of D1 media and 0.2% agarose was added to each well and incubated at 37°C + 5% CO2 for 48 hours. Cells were then fixed with 2 mL of 10% Formaldehyde solution and incubated at room temperature for 30 minutes. The overlay was removed, and cells stained with 1mL of Crystal Violet (BD Biosciences, Franklin Lakes, NJ) per well for 20 minutes. Lastly, each well was washed with 1mL of PBS and the number of plaques in each well were recorded.

$$({}^{PFU}/_{mL} = \frac{\#\ of\ plaques}{dilution\ factor\ x\ sample\ added}$$

2.5.5 Histology

At the indicated time points, three whole lung and accessory lobes were collected per group and fixed in 10% Neutral Buffer Formalin (NBF) for 24 hours. The fixed lung samples were embedded in paraffin and sectioned by the University of Washington histology core. Blinded slides were sent to Colorado State University and stained with hematoxylin and eosin (H&E) then analyzed by veterinary pathologist Dr. Brendan Podell as previously published (141, 159). H&E stained sections were scanned at 20X magnification using an Olympus VS120 microscope, Hamamatsu ORCA-R2 camera, and Olympus VS-ASW 2.9 software. Visiopharm software was used for image analysis. For each tissue section, a region of interest (ROI) was generated at a low magnification with a custom tissue detecting algorithm using decision forest training and classification to differentiate tissue versus background based on color and area. Lesions were identified within tissue ROIs at a high magnification with an additional custom-made algorithm

using decision forest training and classification based on staining intensity, color normalization and deconvolution, area, and morphological features. Percent lesion calculations were integrated into the same algorithm and calculated from tissue area and lesion area as designated by the ROI and lesions detected. Lesion identification and quantification were then reviewed by Dr. Podell (141, 159).

2.5.6 Flow cytometry

Cell populations within the lung were measured kinetically utilizing methods previously published (159). Briefly, lung homogenates were incubated in RBC lysis buffer (eBioscience/Thermo Fischer Scientific), washed and resuspended in RPMI 1640 + 10% FBS, and then evenly dispensed into 96-well round bottom plates. Cells were stained for surface markers with fluorochrome-conjugated monoclonal antibodies against mouse Ly6G (FITC, clone 1A8, Biolegend), Ly6C (PerCP-Cy5.5, clone HK1.4, eBioscience), MHCII I-A/I-E (eF450, clone M5/114.15.2, Invitrogen), CD11c (Bv510, clone N418, Biolegend), CD3 (Bv650, clone 17A2, Biolegend), CD19 (APC, clone 6D5, Biolegend), CD11b (Alexa700, clone M1/70, eBioscience), NK1.1 (PE, clone PK136, eBioscience), CD64 (PE-Cy7, clone X54-5/7.1, Biolegend) and 1 µg/mL of Fc receptor block anti-CD16/CD32 (clone 93, eBioscience) in PBS with 1% bovine serum albumin (BSA) for 15 minutes at room temperature. Samples were washed and before removing samples from the BSL3, samples were incubated in 4% paraformaldehyde for 30 minutes. After wash and resuspension in PBS + 1% BSA, cells were acquired on a BD Bioscience LSRII flow cytometer (BD Bioscience) and analyzed using FlowJo version 10.8.1 (BD Bioscience).

2.5.7 Cytokine Measurement

Bronchoalveolar lavage fluid (BALF) was collected by flushing lungs with 1X PBS, then centrifuged at 400g for 7 minutes to remove cellular debris and filtered. The processed BALF was used in the Meso Scale Discovey (MSD) V-PLEX Proinflammatory Panel 1 Mouse kit (#K15048D), V-PLEX Cytokine Panel 1 Mouse Kit (#K15245D) and U-PLEX Interferon Combo 1

(#K15320K) to measure cytokine levels on the MESO QuickPlex SQ 120MM (Meso Scale Diagnostics, Rockville, MD). For similar in vitro endpoints from cultured Calu-3 supernatants, an MSD human U-PLEX Viral Combo 1 kit was used (#K15343K-1).

2.5.8 In vivo RT-qPCR

Accessory lung lobes from mice at specified time points post SARS-CoV-2 co-infection were harvested and homogenized in 900µL of Qiazol, followed by RNA extraction using the QIAGEN RNeasy Plus Universal mini kit according to the manufacturer's protocol (QIAGEN, Hilden, Germany). RNA was eluted into 30µl. RNA concentration and quality was determined using the NanoDrop 8000 (Thermo Fisher Scientific) and stored at -80°C until assayed. The obtained RNA was then utilized in the High-Capacity RNA-to-cDNA kit for cDNA synthesis using SuperScript™ IV Reverse Transcriptase (Thermo Fisher Scientific), containing a reverse transcriptase with a high-fidelity enzyme following manufacture protocol.

For Fluidigm Real-Time PCR and Dynamic Array IFC (Integrated Fluidic Circuit) Setup, specific target amplification (STA) was done as per the manufacturer's recommendations as the initial step (pre-amplification of cDNA) for the Biomark HD system (Standard BioTools, formerly Fluidigm) carried out on the Standard BioTools 48.48 Gene Expression (GE) Dynamic Array integrated fluidic circuit (IFC) (161). Assay-sets (primers only) were combined as a delta gene multiplex pool (see Appendix supplementary data A.3). Preamplification was carried out for each cDNA sample against a reaction-set. Exonuclease I was then used to clean up the preamplification reactions.

Subsequently, the Biomark Chip was primed, and assay premix for each target was aspirated into the IFC assay inlets for a final concentration of 9 µM primers and 2.5 µM probe per reaction, and pre-amplified samples were aspirated into sample inlets. The IFC was then run in the Biomark HD thermocycler, using the manufacturer-supplied thermal cycling conditions. Results were analyzed using the Fluidigm Real-time PCR Analysis software, where thresholds were manually defined, the baseline was automatically assigned, and a Cycle of quantification

(Cq) cut-off value of 38 was applied. The cycle threshold (Ct) values for the candidate housekeeping gene, RPL13, and target genes were obtained, and delta-delta CT values were calculated.

2.5.9 In vitro experiments

For the in vitro experiments, frozen human peripheral blood mononuclear cells (PBMCs) and whole blood were procured from Bloodworks Northwest (Seattle, WA). PBMCs were thawed, counted, and resuspended to a concentration of 2x106 cells/mL, then rested overnight in RPMI media supplemented with 10% FBS and 1% penicillin/streptomycin at 37 °C + 5% CO2. Cells were counted the next day and viability was assessed before being adjusted to a concentration of 1.5x106 viable cells/mL. Subsequently, the cells were infected with M.tb HN878 at a multiplicity of infection (MOI) of 1 and incubated for 96 hours. Following infection, the cells were centrifuged at 700g for 3 minutes, and the supernatants were collected and filtered through a 0.22-micron filter. Vero or Calu-3 cells were plated and treated with supernatants for 24 hours at 37°C + 5% CO2. Media-only treated cells were used as controls. Post-treatment, the cells were challenged with 75 PFU of SARS-CoV-2 Beta, and plaques were recorded 48 hours post-infection using the viral titer PFA described above.

To assess mRNA expression in cultured cells, RNA was extracted from cultured Calu-3 cells using the QIAGEN RNeasy Plus Universal mini kit. The cells were harvested using 900µL of Qiazol, followed by RNA isolation and cDNA synthesis employing the High-Capacity RNA-to-cDNA kit. RNA and cDNA concentration and quality was determined using the NanoDrop 8000 (Thermo Fisher Scientific) and stored at -80°C until assayed. Quantification of mRNA levels was performed using the GoTaq qPCR and RT-qPCR Systems kit from Promega, following the manufacturer's protocol, and the StepOne Plus Real-Time PCR System (Thermo Fisher Scientific). The mRNA expression levels of Calu-3 cells are presented as Log2 fold change (FC) compared to media-only treated cells and normalized to the housekeeping gene, Beta Actin.

Primers used were selected from published sequences in PrimerBank (RRID:SCR_006898) (see Appendix supplementary data A.6).

2.5.10 Neutralization assay

For neutralization studies, PBMCs were thawed and counted as described previously. PBMCs were plated in 12-well plates at $2.25x10^6$ cells/mL in one mL of RPMI media supplemented with 10% FBS and 1% penicillin/streptomycin. Neutralizing antibodies for human CD4 (BE0351, BioXcell), Lebanon, NH), CD8α (BE0004-2, BioXcell), CD314 (BE0288, BioXcell), and relevant isotype controls, mouse IgG1(BE0083, BioXcell), and mouse IgG2 (BE0085, BioXcell) were then administered at 10µg/mL, 20µg/mL and 100µg/mL in 1 mL. PBMCs and neutralizing antibodies were incubated for 1 hour at 37 °C + 5% CO2 prior to infection with M.tb HN878 at MOI of 1 for 96 hours. For IFNγ neutralization, the IFNγ antibody (BE0235, BioXcell) was added directly to the supernatant from PBMCs infected with M.tb HN878 at 10µg/mL, 20µg/mL and 100µg/mL escalating doses. After infection, supernatants were filtered through a 0.22-micron filter. Vero cells were treated with filtered PBMC supernatants for 24 hours, then challenged with 75 PFU of SARS-CoV-2 Beta, and plaques were recorded 48 hours post-infection using the viral titer PFA described above.

2.5.11 Statistical analysis

Survival analysis was based on the Mantel-Cox log-rank test with Bonferroni correction for multiple comparisons and carried out using GraphPad Prism 9.3.1 (GraphPad Software, San Diego, CA). The bacterial burden, viral titers, cytokine levels, and cell populations (percent frequency and counts) were assessed at a single time point using one-way ANOVA with Tukey's multiple comparison test to compare infection groups. Flow cytometry data was assessed using FlowJo v10.8.1 (BD) and statistical analyses were performed using GraphPad Prism 9.3.1 software. The graphics were made with Biorender. Heat maps of in vivo mRNA expression were created with RStudio using 'pheatmap' function. P values < 0.05 were considered significant and

labeled accordingly in each of the figures (* = P<0.05, **= P<0.01, ***=P<0.001, ****= P<0.0001). Outliers were identified using Grubbs' test at alpha 0.05.

2.6 Acknowledgements

This project has been funded in whole or in part with Federal funds from the National Institute of Allergy and Infectious Diseases, National Institutes of Health, Department of Health and Human Services, under Contract No. 75N93021C00029 (to RNC), Grant R01AI125160 (to RNC and SLB) and additional funding from Seattle Tuberculosis Research Advancement Center under award P30 AI168034 (to RNC). BDW was supported through the National Institutes of Health Training grant to the University of Washington, Diseases of Public Health Importance No. AI00750922 and the Achievement Rewards for College Scientists (ARCS) foundation.

We want to express our gratitude to the committed vivarium personnel for their exceptional care of the animals throughout this study. The following reagents were obtained through BEI Resources by the Coler Lab, NIAID, NIH: Mycobacterium tuberculosis, Strain HN878, NR-13647.

2.7 Author contributions

BDW, conceptualization, formal analysis, investigation, project administration, resources visualization, writing-original draft. DF, investigation, visualization, writing-review and editing. HFMA, formal analysis, investigation, writing-review and editing. BJB, conceptualization, writing-review and editing. BKP, formal analysis, investigation, visualization, writing-review and editing. SEL, conceptualization, supervision, writing-review and editing. SLB, conceptualization, funding acquisition, project administration, supervision, writing-review and editing. RNC, conceptualization, funding acquisition, project administration, supervision, writing-review and editing. All authors contributed to the article and approved the submitted version.

CHAPTER 3. CONCLUSIONS AND FUTURE PERSPECTIVES

3.1. Summary

In this thesis, I developed and characterized a M.tb and SARS-CoV-2 model. Upon characterization the co-infected model exhibited a protective phenotype compared to the SARS-CoV-2-only model. Given the co-infected model was first infected with M.tb it was probable that the established immune response elicited by the M.tb infection prior to co-infection with SARS-CoV-2 could be providing protection against SARS-CoV-2. This thesis describes experiments aimed at investigating the immune mechanism that could be providing this protective phenotype within our coinfection model.

In this thesis, I show that M.tb infection can induce a robust innate response, especially IFNγ. IFNs, including type I-III IFNs have been shown to promote antiviral environments to restrict viral activity. In this work I propose that IFNγ produced from M.tb infection can induce ISG expression, creating an anti-viral environment and dampening secondary SARS-CoV-2 infection severity. This work supports a model in which an existing infection can aid in priming the immune response that upon a secondary immune response help contain and lessen its severity. By exploring factors that can affect either infection we can better understand the complex interactions of M.tb and SARS-CoV-2 co-infection. Additionally, by continuing investigation in characterizing our co-infection we can further elucidate and validate the protective phenotype witnessed in our co-infection model. Here, I present possible areas of further investigation and proposed experiments, which are summarized in **Table 3.1**.

Question	**Experimental strategy**
Does timing and type of M.tb infection affect co-infection with SARS-CoV-2?	• Assess ULDA/VLDA M.tb infections • Investigate different TB stage
What roles do IFNs in M.tb and SARS-CoV-2 co-infection?	• Expand IFN measurements in mouse and human samples • Neutralize IFNs *in vivo* and *in vitro*
What is the function of identified ISGs in providing protection	• Expand ISG expression measurements • Conduct functional assays
What long term effects does co-infection have on TB outcomes?	• Assess later timepoints in animals for disease burden • Measure if alterations in adaptive responses

Do comorbidities affect co-infection outcomes?	• Investigate co-infection in aged mice • Investigate co-infection in obese mice

Table 3.1*. Future experimental strategies*

3.2. Limitations of the study

We acknowledge the limitations within this study and outline how these can be addressed in future experimental strategies. One limitation involves the measurement of IFN proteins, which can be variable and unreliable. To mitigate this, future experiments will expand IFN RNA measurements to validate the observed trends from measured IFN protein levels. Additionally, we emphasize the importance of including measurements of multiple IFN subsets to provide a more comprehensive understanding.

In this study, we also investigate the protective role of IFNγ against SARS-CoV-2. While our focus was on IFNγ's role in inducing ISG expression and creating an antiviral environment, we recognize that IFNγ activates several mechanisms that may contribute to viral protection. Moreover, given the extensive overlap in IFN activity, further studies are required to confirm the specific role of IFNγ in this context.

Despite these limitations, this study is the first to establish a preclinical co-infection mouse model using the clinically virulent strain M.tb HN878 and the SARS-CoV-2 Beta variant of concern, alongside a translational human PBMC in vitro co-infection model. This approach provides novel insights into the complex interactions between M.tb and SARS-CoV-2 during co-infection.

3.3. Exploring how timing and type of M.tb infection mouse model can affect co-infection with SARS-CoV-2

For our co-infection model we utilized a low-dose aerosol (LDA) M.tb infection model. This specific model has been well studied within the TB field and within our own lab (141, 159). With this model, mice are infected with 50-100 CFU, this manifesting into an accelerated disease with robust immune responses diffuse bilaterally throughout the lung, conducive of a more chronic active stage of infection. While this model has been ideal to study TB disease and host response

there are concerns whether it truly recapitulates human TB pathology, which more likely results from infection from a single bacillus (155). In response to this concern there has been the development of the ultra-low-dose aerosol (ULDA) M.tb infection model, where 1-3 CFU are delivered to mice (155). With ULDA, mice develop more organized lesions like the granuloma see in humans, a pathology not witnessed in LDA models. Given the unique characteristic of the granuloma and the important role it plays in both pathology and the host response, investigating how the ULDA model with co-infection fares in comparison to the LDA model we use may give further context to whether different stages of active TB disease (chronic vs. acute) can result to different outcomes with SARS-CoV-2 infection. In addition, given there is a spectrum of TB disease there is still the question whether the stage of TB (latent, subclinical, active) can also affect outcomes in co-infection with SARS-CoV-2. Due to limitations in clinical studies, there haven't been clear conclusions on the effects of the stage of TB. As previously mentioned, a study conducted in India did find that LTBI was negatively correlated to COVID-19 mortality. However, due to its small cohort size further studies are needed to confirm its finding. There have been great strides in developing mouse models which cover the spectrum of TB disease. Kupz et. al. developed a contained M.tb infection (CMTB) mouse model which contains M.tb infection and believed to model individuals with asymptomatic infection who are also able to contain infection (162). For the mouse model M.tb is delivered intradermally to the ear. The bacteria remain within the ear draining lymph node and can be activated with CD4+ T-cell depletion as seen in M.tb and HIV co-infection (162). Nemeth et. al. also showed that challenging the CMTB mouse model with aerosol M.tb led to protection (163).

We conducted a small pilot study co-infecting the CMTB mouse model with SARS-CoV-2 (**Figure B.1**). Female, 6–8-week-old K18-hACE2 mice were administered 10,000 CFU of M.tb HN878 in 10μL intradermally. Six weeks after M.tb administration, mice with either mock-infected with saline or infected with 200 PFU of SARS-CoV-2 Beta, intranasally. After co-infection mice were weighed twice daily and measured for morbidity conferred by 20% weight loss. Interestingly,

we did not witness the same survival increase for the co-infected group compared to the SARS-CoV-2 only groups as we did in the LDA M.tb and SARS-CoV-2 co-infected group. We would like to repeat this study to confirm our findings and expand it to measure if the bacterial burden is affected overtime. In all, this study elucidates the importance of an active immune response already established in the lung to confer protection against secondary SARS-CoV-2 infection.

3.4. What roles do IFNs play in M.tb and SARS-CoV-2 co-infection

In this study, I quantified local mucosal levels of IFNα, IFNβ, and IFNγ in mouse BALF samples, with these findings further corroborated by lung PCR analysis. While we focused on key IFN subtypes in this study, expanding the range of subtypes measured in future work could provide deeper insights into the mechanisms of the induced immune response. Although all type I IFN subsets bind to IFNAR to initiate signaling, they have been shown to exhibit distinct biological activities in both humans and mice (164). By expanding our protein and RNA analyses to include all mouse IFNα subtypes (IFNα1-13, IFNαA, IFNαB), we could enhance our measurements and more precisely determine the abundance of each subtype induced during the infections (164).

Moreover, given the robust nature of M.tb infection and the dynamics of co-infection, it is possible that measuring only global lung responses may have obscured certain signals. Integrating more sensitive techniques such as single-cell RNA sequencing could help pinpoint the activity of specific cell types, potentially revealing subsets that upregulated type I IFN but were undetected in our global measurements. Additionally, this approach could help identify the specific cells driving IFNγ responses, which we sought to characterize in our in vitro neutralization studies (**Figure 2.9**).

Although our study did not primarily focus on IFNλ subsets (IFNλ2, IFNλ3), we did measure its RNA expression in the in vitro studies (**Figure 2.7**), though it was not assessed in our mouse model. Measuring IFNλ protein and RNA levels in mouse BALF samples could reveal whether it works synergistically with IFNγ to establish an antiviral environment in the lung. Similar to type I IFNs, IFNλ has known antiviral properties, inducing the expression of ISGs and activating

and recruiting immune cells (165, 166). However, unlike type I and II IFNs, the IFNλ receptor (IFNLR) is not ubiquitously expressed; it is primarily found on epithelial barrier cells and a subset of immune cells, including neutrophils, macrophages, and plasmacytoid dendritic cells (DCs). This selective expression may help prevent the hyperinflammation often associated with type I and II IFNs (165, 167). IFNλ has demonstrated protective effects against SARS-CoV-2, with a clinical study reporting higher IFNλ1 and IFNλ3 expression in the upper airways of mildly ill patients compared to those with severe COVID-19 (168). Furthermore, direct IFNλ treatment has been shown to protect against severe SARS-CoV-2 infection outcomes in both mice and humans (169, 170) Although the role of IFNλ in M.tb infection is not fully understood, its presence has been detected in the sputum of individuals with active TB (171). Given the overlap in signaling pathways among type I, II, and III IFNs, co-expression—albeit at different levels—is anticipated.

To determine whether IFNs are working synergistically or if IFNγ alone is driving the protection observed in our co-infection models, further in vitro and in vivo neutralization studies are needed. For in vivo studies, M.tb-infected animals would receive neutralizing antibodies against IFNGR, IFNAR, or IFNLR administered intranasally (mucosally) or intraperitoneally (systemically) just prior to SARS-CoV-2 infection, thereby inhibiting the corresponding IFN activity. Survival rates and viral burden would then be measured and compared with non-treated co-infected animals and singly infected animals. This would help determine whether the protective phenotype is abrogated by neutralization and clarify the role each IFN plays in protection against SARS-CoV-2. A short treatment regimen with neutralizing antibodies would be necessary to prevent exacerbation of M.tb infection and to avoid introducing new variables to the model.

For *in vitro* studies, I had conducted neutralization experiments targeting IFNγ (**Figure 2.9**), which demonstrated a loss of protection when IFNγ was neutralized. The study could be extended by incorporating neutralizing antibodies against IFNα, IFNβ, and IFNλ to assess the roles of type I and III IFNs.

3.5. What is the function of identified ISGs in providing protection

In this study, we identified specific ISGs that are upregulated in epithelial cells following M.tb-induced cytokine treatment, confirming their expression. However, the question remains as to whether, and how, these ISGs contribute to restricting SARS-CoV-2 activity in this co-infection model. To address this, a comprehensive approach could be employed. First, a microarray analysis could be conducted on epithelial cells treated with cytokines derived from M.tb-infected PBMCs, likely expanding the scope of ISGs identified as being upregulated. Once these ISGs are identified, their antiviral activity can be systematically evaluated using various techniques.

One approach is a small interfering RNA (siRNA) screening assay(172, 173), where pre-treated epithelial cells are transfected with siRNAs targeting specific ISGs, followed by a challenge with SARS-CoV-2. Viral titers would then be measured to assess the impact of silencing each ISG. If a particular ISG is crucial for inhibiting viral activity, we would expect to see a loss of protection when it is silenced. Alternatively, a gain-of-function assay could be employed (174), in which the identified ISGs are endogenously expressed in epithelial cells, which are then challenged with SARS-CoV-2. In this scenario, a decrease in viral titers would be expected if the expressed ISG effectively inhibits viral replication.

It is important to note that identifying individual ISGs with significant antiviral activity may be challenging due to the potential combinatorial effects of ISGs, where the collective action of multiple ISGs is necessary for robust antiviral defense. Consequently, individual ISGs may not show significant inhibition of viral activity when expressed alone (172). If no substantial changes in viral titer are observed in either assay, it would be prudent to investigate combinations of ISGs to determine whether they exert a synergistic effect in restricting SARS-CoV-2 replication. Overall, this multifaceted approach will help elucidate the specific roles of ISGs in the context of M.tb and SARS-CoV-2 co-infection, potentially revealing new therapeutic targets for enhancing antiviral immunity.

3.6. Long term effects SARS-CoV-2 co-infection has on TB outcomes

For this thesis I focused primarily on the acute stage of M.tb and SARS-CoV-2 infection to observe the SARS-CoV-2 infection course. Lung pathology and CFU were measured to assess the TB disease outcomes within our mouse model. There were no significant changes found in bacterial burden to suggest TB disease outcome was exacerbated by co-infection during the acute timeline captured. However, there is a question of whether the effects of co-infection would be witnessed during the chronic stages of M.tb infection. Interestingly, in a M.tb and IAV co-infection study in which the authors reported co-infection worsened TB outcomes, increase in bacterial burden wasn't measured until 120 days post-co-infection, well into chronic stage of infection (86). Therefore, it is possible M.tb co-infection with a virus can induce a change in the immune response that leads to worsened protection over time. However, the study also reported a significant decrease in survival between the co-infected group and M.tb only group (86). We did not see this trend with our long-term survival outcomes. There was no significant difference in survival between the co-infected and M.tb only group (**Figure B.2**). Additionally, measured lung pathology showed to be reduced in the M.tb and SARS-CoV-2 co-infected group compared to the M.tb-only group at the later 14-day post-co-infection timepoint (35 days post M.tb infection) (**Figure 2.2E**), which could potentially provide evidence of TB outcomes not worsening with co-infection, but further research is needed to validate these findings. Given these contrasts, we could infer that M.tb may dampen the effects of SARS-CoV-2 viral replication and associated immunopathology, potentially leading to less exacerbation of TB outcomes compared to IAV and M.tb co-infection. However, it is crucial to measure outcomes at the chronic stage to confirm this hypothesis. Additionally, if there is a significant change in TB burden during later chronic time points, we might expect alterations in the adaptive immune response, such as antibody production or memory responses. Therefore, it is vital to assess whether co-infection modifies M.tb-specific adaptive responses, providing a comprehensive understanding of the interplay between these pathogens

3.7. Potential for comorbidities to affect co-infection outcomes

While SARS-CoV-2 has affected all populations, individuals with comorbidities have disproportionately experienced severe disease progression (175, 176). Factors such as obesity, age, sex, metabolic disorders, and chronic diseases have been identified as high-risk factors for SARS-CoV-2 infection and increased COVID-19 severity (175, 176). It has been hypothesized that the elevated risk associated with obesity and age may be due not only to underlying metabolic and inflammatory dysregulation but also to a higher likelihood of harboring other chronic conditions. These conditions, such as diabetes, hypertension, and heart disease, are also risk factors for severe SARS-CoV-2 outcomes (176). Immune profiling of COVID-19 patients with pre-existing conditions found that those with chronic kidney disease displayed an overactive, exhausted T cell compartment and less active innate immune response (177). Those with heart disease and lung disease were associated with a hyperactive, exhausted NK and T cell compartments (177). While male sex is a risk factor for severe COVID-19 disease outcomes accompanied with increased hospitalization rates and slower viral clearance, the underlying immune dysregulation that could be promoting it is still widely unknown (178).

Similarly, age, sex, and metabolic disorders, including diabetes, are recognized as risk factors for TB progression (179). The increased TB burden among individuals with diabetes has been linked to defects in early bacterial detection and impaired immune cell activation, which can compromise downstream adaptive immune responses (180). Males with TB have been shown to exhibit higher sputum culture loads and smear positivity rates, which are associated with lower IgM antibody responses compared to females (181). While hormones are thought to drive these sex-based differences in TB outcomes, further research is needed to clarify the distinct immune responses to TB in males and females. Clinical findings, though mixed on the risk of co-infection, have highlighted the significant influence of age and comorbidities on disease outcomes (84).

Given the importance of comorbidities in influencing M.tb and SARS-CoV-2 infection outcomes, it is crucial to further investigate how these conditions might alter immune responses and co-infection outcomes. Our findings demonstrate that an established immune response to

M.tb infection can prime the environment before co-infection with SARS-CoV-2. However, we hypothesize that in the context of pre-existing conditions that dampen or dysregulate the immune response to the initial M.tb infection, this priming effect and its protective nature may be lost during co-infection.

To test this, aged mice and mice with metabolic disorders (e.g., diabetes, obesity) could be incorporated into the M.tb and SARS-CoV-2 co-infection model to assess how these conditions influence immune responses and disease outcomes. Additionally, although our co-infection survival curve included both male and female mice and did not reveal any significant differences, the following characterization was conducted exclusively in female mice. It would be important to extend this characterization to male mice, given that sex can influence immune responses, and males are known to have differing outcomes in both M.tb and SARS-CoV-2 infections. By investigating the effects of age, sex and obesity in the context of co-infection, we can develop comorbidity animal models to determine whether immune dysregulation is exacerbated by these conditions and whether it correlates with TB and COVID-19 disease progression.

3.8. Concluding remarks

M.tb and SARS-CoV-2 are two highly prevalent pathogens that continue to pose significant public health challenges globally. Despite considerable progress in managing and mitigating the impact of these infections, both remain considerable causes of morbidity and mortality, particularly among vulnerable populations. The persistence of these pathogens underscores the need for a deeper understanding of their interactions, especially in the context of co-infection, which can complicate disease progression and treatment outcomes.

The interaction of M.tb and SARS-CoV-2 presents a unique challenge, as both pathogens elicit complex immune responses that can influence one another. Understanding these dynamics is crucial for developing tailored strategies to prevent and manage co-infections. Additionally, this knowledge could guide public health policies and clinical practices, ensuring that high-risk

populations receive the most effective care. Ultimately, our aim is to advance understanding in this area, with the hope of improving outcomes and reducing the global burden of these diseases.

BIBLIOGRAPHY

1. Organization WH. Global tuberculosis report 2020. . Geneva: Licence: CC BY-NC-SA 3.0 IGO . ; 2020.
2. Organization WH. Global tuberculosis report 2023. Geneva2023.
3. Drancourt ECaM. Steps towards the discovery of Mycobacterium tuberculosis by Robert Koch, 1882. Clinical Microbiology and Infection. 2014;20(3):196-201.
4. The evidence for the incidence of tuberculosis in ancient Egypt. British Journal of Tuberculosis. 1939;33(3):142-52.
5. Meehan CJ, Barco RA, Loh YE, Cogneau S, Rigouts L. Reconstituting the genus Mycobacterium. Int J Syst Evol Microbiol. 2021;71(9).
6. Bespiatykh D, Bespyatykh J, Mokrousov I, Shitikov E. A Comprehensive Map of Mycobacterium tuberculosis Complex Regions of Difference. mSphere. 2021;6(4):10.1128/msphere.00535-21.
7. Bañuls AL, Sanou A, Van Anh NT, Godreuil S. Mycobacterium tuberculosis: ecology and evolution of a human bacterium. J Med Microbiol. 2015;64(11):1261-9.
8. Click ES, Moonan PK, Winston CA, Cowan LS, Oeltmann JE. Relationship Between Mycobacterium tuberculosis Phylogenetic Lineage and Clinical Site of Tuberculosis. Clinical Infectious Diseases. 2012;54(2):211-9.
9. Phyu AN, Aung ST, Palittapongarnpim P, Htet KKK, Mahasirimongkol S, Aung HL, et al. Distribution of Mycobacterium tuberculosis Lineages and Drug Resistance in Upper Myanmar. Trop Med Infect Dis. 2022;7(12).
10. Freschi L, Vargas R, Husain A, Kamal SMM, Skrahina A, Tahseen S, et al. Population structure, biogeography and transmissibility of Mycobacterium tuberculosis. Nature Communications. 2021;12(1):6099.
11. Fenner L, Egger M, Bodmer T, Furrer H, Ballif M, Battegay M, et al. HIV Infection Disrupts the Sympatric Host–Pathogen Relationship in Human Tuberculosis. PLOS Genetics. 2013;9(3):e1003318.
12. Yang J, Zhang L, Qiao W, Luo Y. Mycobacterium tuberculosis: Pathogenesis and therapeutic targets. MedComm (2020). 2023;4(5):e353.
13. Mayer-Barber KD, Barber DL. Innate and Adaptive Cellular Immune Responses to Mycobacterium tuberculosis Infection. Cold Spring Harb Perspect Med. 2015;5(12).
14. Jo EK. Mycobacterial interaction with innate receptors: TLRs, C-type lectins, and NLRs. Curr Opin Infect Dis. 2008;21(3):279-86.
15. Hossain MM, Norazmi MN. Pattern recognition receptors and cytokines in Mycobacterium tuberculosis infection--the double-edged sword? Biomed Res Int. 2013;2013:179174.
16. Tapping RI, Tobias PS. Mycobacterial lipoarabinomannan mediates physical interactions between TLR1 and TLR2 to induce signaling. J Endotoxin Res. 2003;9(4):264-8.
17. Bulut Y, Michelsen KS, Hayrapetian L, Naiki Y, Spallek R, Singh M, et al. Mycobacterium tuberculosis heat shock proteins use diverse Toll-like receptor pathways to activate pro-inflammatory signals. J Biol Chem. 2005;280(22):20961-7.
18. Ohashi K, Burkart V, Flohé S, Kolb H. Cutting edge: heat shock protein 60 is a putative endogenous ligand of the toll-like receptor-4 complex. J Immunol. 2000;164(2):558-61.
19. Ahmad F, Rani A, Alam A, Zarin S, Pandey S, Singh H, et al. Macrophage: A Cell With Many Faces and Functions in Tuberculosis. Front Immunol. 2022;13:747799.

20. Rajaram MV, Ni B, Dodd CE, Schlesinger LS. Macrophage immunoregulatory pathways in tuberculosis. Semin Immunol. 2014;26(6):471-85.
21. Larsen SE, Williams BD, Rais M, Coler RN, Baldwin SL. It Takes a Village: The Multifaceted Immune Response to Mycobacterium tuberculosis Infection and Vaccine-Induced Immunity. Front Immunol. 2022;13:840225.
22. Leemans JC, Thepen T, Weijer S, Florquin S, van Rooijen N, van de Winkel JG, et al. Macrophages play a dual role during pulmonary tuberculosis in mice. J Infect Dis. 2005;191(1):65-74.
23. Flynn JL, Chan J. Immune evasion by Mycobacterium tuberculosis: living with the enemy. Curr Opin Immunol. 2003;15(4):450-5.
24. Gengenbacher M, Kaufmann SH. Mycobacterium tuberculosis: success through dormancy. FEMS Microbiol Rev. 2012;36(3):514-32.
25. Cohen SB, Gern BH, Delahaye JL, Adams KN, Plumlee CR, Winkler JK, et al. Alveolar Macrophages Provide an Early Mycobacterium tuberculosis Niche and Initiate Dissemination. Cell Host Microbe. 2018;24(3):439-46.e4.
26. James BW, Williams A, Marsh PD. The physiology and pathogenicity of Mycobacterium tuberculosis grown under controlled conditions in a defined medium. J Appl Microbiol. 2000;88(4):669-77.
27. Urdahl KB, Shafiani S, Ernst JD. Initiation and regulation of T-cell responses in tuberculosis. Mucosal Immunology. 2011;4(3):288-93.
28. Pawlowski A, Jansson M, Sköld M, Rottenberg ME, Källenius G. Tuberculosis and HIV co-infection. PLoS Pathog. 2012;8(2):e1002464.
29. Yao S, Huang D, Chen CY, Halliday L, Wang RC, Chen ZW. CD4+ T cells contain early extrapulmonary tuberculosis (TB) dissemination and rapid TB progression and sustain multieffector functions of CD8+ T and CD3- lymphocytes: mechanisms of CD4+ T cell immunity. J Immunol. 2014;192(5):2120-32.
30. Lin PL, Rutledge T, Green AM, Bigbee M, Fuhrman C, Klein E, et al. CD4 T cell depletion exacerbates acute Mycobacterium tuberculosis while reactivation of latent infection is dependent on severity of tissue depletion in cynomolgus macaques. AIDS Res Hum Retroviruses. 2012;28(12):1693-702.
31. Flory CM, Hubbard RD, Collins FM. Effects of in vivo T lymphocyte subset depletion on mycobacterial infections in mice. J Leukoc Biol. 1992;51(3):225-9.
32. Leveton C, Barnass S, Champion B, Lucas S, De Souza B, Nicol M, et al. T-cell-mediated protection of mice against virulent Mycobacterium tuberculosis. Infect Immun. 1989;57(2):390-5.
33. Lyadova IV, Panteleev AV. Th1 and Th17 Cells in Tuberculosis: Protection, Pathology, and Biomarkers. Mediators Inflamm. 2015;2015:854507.
34. Torrado E, Cooper AM. IL-17 and Th17 cells in tuberculosis. Cytokine Growth Factor Rev. 2010;21(6):455-62.
35. Pai M, Behr MA, Dowdy D, Dheda K, Divangahi M, Boehme CC, et al. Tuberculosis. Nature Reviews Disease Primers. 2016;2(1):16076.
36. Zumla A, Raviglione M, Hafner R, von Reyn CF. Tuberculosis. N Engl J Med. 2013;368(8):745-55.
37. Lee J, Repasy T, Papavinasasundaram K, Sassetti C, Kornfeld H. Mycobacterium tuberculosis induces an atypical cell death mode to escape from infected macrophages. PLoS One. 2011;6(3):e18367.

38. Sholeye AR, Williams AA, Loots DT, Tutu van Furth AM, van der Kuip M, Mason S. Tuberculous Granuloma: Emerging Insights From Proteomics and Metabolomics. Front Neurol. 2022;13:804838.
39. Cardona PJ, Llatjós R, Gordillo S, Díaz J, Ojanguren I, Ariza A, et al. Evolution of granulomas in lungs of mice infected aerogenically with Mycobacterium tuberculosis. Scand J Immunol. 2000;52(2):156-63.
40. Ramakrishnan L. Revisiting the role of the granuloma in tuberculosis. Nat Rev Immunol. 2012;12(5):352-66.
41. Boom WH, Schaible UE, Achkar JM. The knowns and unknowns of latent Mycobacterium tuberculosis infection. J Clin Invest. 2021;131(3).
42. Houben RM, Dodd PJ. The Global Burden of Latent Tuberculosis Infection: A Re-estimation Using Mathematical Modelling. PLoS Med. 2016;13(10):e1002152.
43. Dong E, Du H, Gardner L. An interactive web-based dashboard to track COVID-19 in real time. Lancet Infect Dis. 2020;20(5):533-4.
44. Chen J. Pathogenicity and transmissibility of 2019-nCoV-A quick overview and comparison with other emerging viruses. Microbes Infect. 2020;22(2):69-71.
45. Sindhuja T, Kumari R, Kumar A. Epidemiology, transmission and pathogenesis of SARS-CoV-2. Computational Approaches for Novel Therapeutic and Diagnostic Designing to Mitigate SARS-CoV-2 Infection: Copyright © 2022 Elsevier Inc. All rights reserved.; 2022. p. 23-42.
46. Gorbalenya AE, Baker SC, Baric RS, de Groot RJ, Drosten C, Gulyaeva AA, et al. The species Severe acute respiratory syndrome-related coronavirus: classifying 2019-nCoV and naming it SARS-CoV-2. Nature Microbiology. 2020;5(4):536-44.
47. Pal M, Berhanu G, Desalegn C, Kandi V. Severe Acute Respiratory Syndrome Coronavirus-2 (SARS-CoV-2): An Update. Cureus. 2020;12(3):e7423.
48. Tabur A, Arslanoğlu A. A 50-Year Overview of the Coronavirus Family with Science Mapping Techniques: A Review. Iran J Public Health. 2021;50(4):649-64.
49. Cascella M, Rajnik M, Aleem A, Dulebohn S, Napoli R. Features, Evaluation, and Treatment of Coronavirus (COVID-19) StatPearls; 2023.
50. Yang H, Rao Z. Structural biology of SARS-CoV-2 and implications for therapeutic development. Nature Reviews Microbiology. 2021;19(11):685-700.
51. Cavanagh D. Coronaviruses in poultry and other birds. Avian Pathol. 2005;34(6):439-48.
52. Hamre D, Procknow JJ. A new virus isolated from the human respiratory tract. Proc Soc Exp Biol Med. 1966;121(1):190-3.
53. Bar-On YM, Flamholz A, Phillips R, Milo R. SARS-CoV-2 (COVID-19) by the numbers. Elife. 2020;9.
54. Zhang Z, Nomura N, Muramoto Y, Ekimoto T, Uemura T, Liu K, et al. Structure of SARS-CoV-2 membrane protein essential for virus assembly. Nature Communications. 2022;13(1):4399.
55. Volz E, Hill V, McCrone JT, Price A, Jorgensen D, O'Toole Á, et al. Evaluating the Effects of SARS-CoV-2 Spike Mutation D614G on Transmissibility and Pathogenicity. Cell. 2021;184(1):64-75.e11.
56. Carabelli AM, Peacock TP, Thorne LG, Harvey WT, Hughes J, de Silva TI, et al. SARS-CoV-2 variant biology: immune escape, transmission and fitness. Nature Reviews Microbiology. 2023;21(3):162-77.

57. Aleem A, Akbar Samad A, Vaqar S. Emerging Variants of SARS-CoV-2 and Novel Therapeutics Against Coronavirus (COVID-19). StatPearls; 2023.
58. Faria NR, Mellan TA, Whittaker C, Claro IM, Candido DDS, Mishra S, et al. Genomics and epidemiology of the P.1 SARS-CoV-2 lineage in Manaus, Brazil. Science. 2021;372(6544):815-21.
59. Gu H, Krishnan P, Ng DYM, Chang LDJ, Liu GYZ, Cheng SSM, et al. Probable Transmission of SARS-CoV-2 Omicron Variant in Quarantine Hotel, Hong Kong, China, November 2021. Emerg Infect Dis. 2022;28(2):460-2.
60. Davies NG, Abbott S, Barnard RC, Jarvis CI, Kucharski AJ, Munday JD, et al. Estimated transmissibility and impact of SARS-CoV-2 lineage B.1.1.7 in England. Science. 2021;372(6538).
61. Tegally H, Wilkinson E, Giovanetti M, Iranzadeh A, Fonseca V, Giandhari J, et al. Detection of a SARS-CoV-2 variant of concern in South Africa. Nature. 2021;592(7854):438-43.
62. Mistry P, Barmania F, Mellet J, Peta K, Strydom A, Viljoen IM, et al. SARS-CoV-2 Variants, Vaccines, and Host Immunity. Frontiers in Immunology. 2022;12.
63. Martines RB, Ritter JM, Matkovic E, Gary J, Bollweg BC, Bullock H, et al. Pathology and Pathogenesis of SARS-CoV-2 Associated with Fatal Coronavirus Disease, United States. Emerg Infect Dis. 2020;26(9):2005-15.
64. Martono, Fatmawati F, Mulyanti S. Risk Factors Associated with the Severity of COVID-19. Malays J Med Sci. 2023;30(3):84-92.
65. Wang CC, Prather KA, Sznitman J, Jimenez JL, Lakdawala SS, Tufekci Z, et al. Airborne transmission of respiratory viruses. Science. 2021;373(6558).
66. Klompas M, Baker MA, Rhee C. Airborne Transmission of SARS-CoV-2: Theoretical Considerations and Available Evidence. Jama. 2020;324(5):441-2.
67. Toyokawa T, Shimada T, Hayamizu T, Sekizuka T, Zukeyama Y, Yasuda M, et al. Transmission of SARS-CoV-2 during a 2-h domestic flight to Okinawa, Japan, March 2020. Influenza Other Respir Viruses. 2022;16(1):63-71.
68. Meyerowitz EA, Richterman A. SARS-CoV-2 Transmission and Prevention in the Era of the Delta Variant. Infect Dis Clin North Am. 2022;36(2):267-93.
69. Lamers MM, Haagmans BL. SARS-CoV-2 pathogenesis. Nature Reviews Microbiology. 2022;20(5):270-84.
70. Barkauskas CE, Cronce MJ, Rackley CR, Bowie EJ, Keene DR, Stripp BR, et al. Type 2 alveolar cells are stem cells in adult lung. J Clin Invest. 2013;123(7):3025-36.
71. Jackson CB, Farzan M, Chen B, Choe H. Mechanisms of SARS-CoV-2 entry into cells. Nature Reviews Molecular Cell Biology. 2022;23(1):3-20.
72. Yin X, Riva L, Pu Y, Martin-Sancho L, Kanamune J, Yamamoto Y, et al. MDA5 Governs the Innate Immune Response to SARS-CoV-2 in Lung Epithelial Cells. Cell Rep. 2021;34(2):108628.
73. Yang DM, Geng TT, Harrison AG, Wang PH. Differential roles of RIG-I like receptors in SARS-CoV-2 infection. Mil Med Res. 8. England: © 2021. The Author(s). 2021. p. 49.
74. Blanco-Melo D, Nilsson-Payant BE, Liu WC, Uhl S, Hoagland D, Møller R, et al. Imbalanced Host Response to SARS-CoV-2 Drives Development of COVID-19. Cell. 2020;181(5):1036-45.e9.
75. Minkoff JM, tenOever B. Innate immune evasion strategies of SARS-CoV-2. Nat Rev Microbiol. 2023;21(3):178-94.

76. Zhang W, Ma Z, Wu Y, Shi X, Zhang Y, Zhang M, et al. SARS-CoV-2 3C-like protease antagonizes interferon-beta production by facilitating the degradation of IRF3. Cytokine. 2021;148:155697.
77. Zhang Q, Chen Z, Huang C, Sun J, Xue M, Feng T, et al. Severe Acute Respiratory Syndrome Coronavirus 2 (SARS-CoV-2) Membrane (M) and Spike (S) Proteins Antagonize Host Type I Interferon Response. Frontiers in Cellular and Infection Microbiology. 2021;11.
78. Alefishat E, Jelinek HF, Mousa M, Tay GK, Alsafar HS. Immune response to SARS-CoV-2 variants: A focus on severity, susceptibility, and preexisting immunity. J Infect Public Health. 2022;15(2):277-88.
79. Min Y-Q, Huang M, Sun X, Deng F, Wang H, Ning Y-J. Immune evasion of SARS-CoV-2 from interferon antiviral system. Computational and Structural Biotechnology Journal. 2021;19:4217-25.
80. Chen Y, Wang Y, Fleming J, Yu Y, Gu Y, Liu C, et al. Active or latent tuberculosis increases susceptibility to COVID-19 and disease severity. medRxiv. 2020:2020.03.10.20033795.
81. Western Cape Department of Health in collaboration with the National Institute for Communicable Diseases SA. Risk Factors for Coronavirus Disease 2019 (COVID-19) Death in a Population Cohort Study from the Western Cape Province, South Africa. Clin Infect Dis. 2021;73(7):e2005-e15.
82. Muflihah H, Yulianto FA, Rina, Sampurno E, Ferdiana A, Rahimah SB. Tuberculosis Coinfection among COVID-19 Patients: Clinical Presentation and Mortality in a Tertiary Lung Hospital in Indonesia. Int J Mycobacteriol. 2024;13(1):58-64.
83. Madan M, Baldwa B, Raja A, Tyagi R, Dwivedi T, Mohan A, et al. Impact of Latent Tuberculosis on Severity and Outcomes in Admitted COVID-19 Patients. Cureus. 2021;13(11):e19882.
84. Stochino C, Villa S, Zucchi P, Parravicini P, Gori A, Raviglione MC. Clinical characteristics of COVID-19 and active tuberculosis co-infection in an Italian reference hospital. Eur Respir J. 56. England2020.
85. Walaza S, Cohen C, Tempia S, Moyes J, Nguweneza A, Madhi SA, et al. Influenza and tuberculosis co-infection: A systematic review. Influenza Other Respir Viruses. 2020;14(1):77-91.
86. Redford PS, Mayer-Barber KD, McNab FW, Stavropoulos E, Wack A, Sher A, et al. Influenza A virus impairs control of Mycobacterium tuberculosis coinfection through a type I interferon receptor-dependent pathway. J Infect Dis. 2014;209(2):270-4.
87. Ring S, Eggers L, Behrends J, Wutkowski A, Schwudke D, Kröger A, et al. Blocking IL-10 receptor signaling ameliorates Mycobacterium tuberculosis infection during influenza-induced exacerbation. JCI Insight. 2019;5(10).
88. Kaufmann E, Khan N, Tran KA, Ulndreaj A, Pernet E, Fontes G, et al. BCG vaccination provides protection against IAV but not SARS-CoV-2. Cell Rep. 2022;38(10):110502.
89. Hatherill M, Cobelens F. Infant BCG vaccination is beneficial, but not sufficient. The Lancet Global Health. 2022;10(9):e1220-e1.
90. O'Neill LAJ, Netea MG. BCG-induced trained immunity: can it offer protection against COVID-19? Nat Rev Immunol. 2020;20(6):335-7.
91. Rivas MN, Ebinger JE, Wu M, Sun N, Braun J, Sobhani K, et al. BCG vaccination history associates with decreased SARS-CoV-2 seroprevalence across a diverse cohort of health care workers. J Clin Invest. 2021;131(2).

92. Pittet LF, Messina NL, Orsini F, Moore CL, Abruzzo V, Barry S, et al. Randomized Trial of BCG Vaccine to Protect against Covid-19 in Health Care Workers. N Engl J Med. 2023;388(17):1582-96.
93. Hilligan KL, Namasivayam S, Clancy CS, O'Mard D, Oland SD, Robertson SJ, et al. Intravenous administration of BCG protects mice against lethal SARS-CoV-2 challenge. J Exp Med. 2022;219(2).
94. Zhang BZ, Shuai H, Gong HR, Hu JC, Yan B, Yuen TT, et al. Bacillus Calmette-Guérin-induced trained immunity protects against SARS-CoV-2 challenge in K18-hACE2 mice. JCI Insight. 2022;7(11).
95. Lowery SA, Sariol A, Perlman S. Innate immune and inflammatory responses to SARS-CoV-2: Implications for COVID-19. Cell Host & Microbe. 2021;29(7):1052-62.
96. McNab F, Mayer-Barber K, Sher A, Wack A, O'Garra A. Type I interferons in infectious disease. Nature Reviews Immunology. 2015;15(2):87-103.
97. Lee AJ, Ashkar AA. The Dual Nature of Type I and Type II Interferons. Frontiers in Immunology. 2018;9.
98. Kotov DI, Lee OV, Fattinger SA, Langner CA, Guillen JV, Peters JM, et al. Early cellular mechanisms of type I interferon-driven susceptibility to tuberculosis. Cell. 2023;186(25):5536-53.e22.
99. Berns SA, Isakova JA, Pekhtereva PI. Therapeutic potential of interferon-gamma in tuberculosis. Admet dmpk. 2022;10(1):63-73.
100. Tau G, Rothman P. Biologic functions of the IFN-gamma receptors. Allergy. 1999;54(12):1233-51.
101. Shirey KA, Jung JY, Maeder GS, Carlin JM. Upregulation of IFN-gamma receptor expression by proinflammatory cytokines influences IDO activation in epithelial cells. J Interferon Cytokine Res. 2006;26(1):53-62.
102. Bhat MY, Solanki HS, Advani J, Khan AA, Keshava Prasad TS, Gowda H, et al. Comprehensive network map of interferon gamma signaling. J Cell Commun Signal. 2018;12(4):745-51.
103. Liu S-Y, Sanchez DJ, Aliyari R, Lu S, Cheng G. Systematic identification of type I and type II interferon-induced antiviral factors. Proceedings of the National Academy of Sciences. 2012;109(11):4239-44.
104. Galani I-E, Rovina N, Lampropoulou V, Triantafyllia V, Manioudaki M, Pavlos E, et al. Untuned antiviral immunity in COVID-19 revealed by temporal type I/III interferon patterns and flu comparison. Nature Immunology. 2021;22(1):32-40.
105. Booysen P, Wilkinson KA, Sheerin D, Waters R, Coussens AK, Wilkinson RJ. Immune interaction between SARS-CoV-2 and Mycobacterium tuberculosis. Front Immunol. 2023;14:1254206.
106. Daneshvar P, Hajikhani B, Sameni F, Noorisepehr N, Zare F, Bostanshirin N, et al. COVID-19 and tuberculosis coinfection: An overview of case reports/case series and meta-analysis of prevalence studies. Heliyon. 2023;9(2):e13637.
107. Motta I, Centis R, D'Ambrosio L, García-García JM, Goletti D, Gualano G, et al. Tuberculosis, COVID-19 and migrants: Preliminary analysis of deaths occurring in 69 patients from two cohorts. Pulmonology. 2020;26(4):233-40.
108. du Bruyn E, Stek C, Daroowala R, Said-Hartley Q, Hsiao M, Schafer G, et al. Effects of tuberculosis and/or HIV-1 infection on COVID-19 presentation and immune response in Africa. Nat Commun. 2023;14(1):188.

109. Casco N, Jorge AL, Palmero DJ, Alffenaar JW, Fox GJ, Ezz W, et al. Long-term outcomes of the global tuberculosis and COVID-19 co-infection cohort. Eur Respir J. 2023;62(5).
110. Aiello A, Najafi-Fard S, Goletti D. Initial immune response after exposure to Mycobacterium tuberculosis or to SARS-COV-2: similarities and differences. Frontiers in Immunology. 2023;14.
111. Najafi-Fard S, Aiello A, Navarra A, Cuzzi G, Vanini V, Migliori GB, et al. Characterization of the immune impairment of patients with tuberculosis and COVID-19 coinfection. Int J Infect Dis. 2023;130 Suppl 1:S34-s42.
112. Sheerin D, Phan TK, Eriksson EM, Coussens AK. Distinct and synergistic immunological responses to SARS-CoV-2 and Mycobacterium tuberculosis during co-infection identified by single-cell-RNA-seq. medRxiv. 2023:2023.05.24.23290499.
113. Tay MZ, Poh CM, Rénia L, MacAry PA, Ng LFP. The trinity of COVID-19: immunity, inflammation and intervention. Nat Rev Immunol. 2020;20(6):363-74.
114. Bortolotti D, Gentili V, Rizzo S, Schiuma G, Beltrami S, Strazzabosco G, et al. TLR3 and TLR7 RNA Sensor Activation during SARS-CoV-2 Infection. Microorganisms. 2021;9(9).
115. Salvi V, Nguyen HO, Sozio F, Schioppa T, Gaudenzi C, Laffranchi M, et al. SARS-CoV-2–associated ssRNAs activate inflammation and immunity via TLR7/8. JCI Insight. 2021;6(18).
116. Yamada T, Sato S, Sotoyama Y, Orba Y, Sawa H, Yamauchi H, et al. RIG-I triggers a signaling-abortive anti-SARS-CoV-2 defense in human lung cells. Nat Immunol. 2021;22(7):820-8.
117. Schiuma G, Beltrami S, Bortolotti D, Rizzo S, Rizzo R. Innate Immune Response in SARS-CoV-2 Infection. Microorganisms. 2022;10(3).
118. Cremoni M, Allouche J, Graça D, Zorzi K, Fernandez C, Teisseyre M, et al. Low baseline IFN-γ response could predict hospitalization in COVID-19 patients. Frontiers in Immunology. 2022;13.
119. Felgenhauer U, Schoen A, Gad HH, Hartmann R, Schaubmar AR, Failing K, et al. Inhibition of SARS-CoV-2 by type I and type III interferons. J Biol Chem. 2020;295(41):13958-64.
120. Hadjadj J, Yatim N, Barnabei L, Corneau A, Boussier J, Smith N, et al. Impaired type I interferon activity and inflammatory responses in severe COVID-19 patients. Science. 2020;369(6504):718-24.
121. Silva BJdA, Krogstad PA, Teles RMB, Andrade PR, Rajfer J, Ferrini MG, et al. IFN-γ-mediated control of SARS-CoV-2 infection through nitric oxide. Frontiers in Immunology. 2023;14.
122. Vanderheiden A, Ralfs P, Chirkova T, Upadhyay AA, Zimmerman MG, Bedoya S, et al. Type I and Type III Interferons Restrict SARS-CoV-2 Infection of Human Airway Epithelial Cultures. J Virol. 2020;94(19).
123. Lazear HM, Schoggins JW, Diamond MS. Shared and Distinct Functions of Type I and Type III Interferons. Immunity. 2019;50(4):907-23.
124. Samuel CE. Interferon at the crossroads of SARS-CoV-2 infection and COVID-19 disease. J Biol Chem. 2023;299(8):104960.
125. Fung SY, Siu KL, Lin H, Yeung ML, Jin DY. SARS-CoV-2 main protease suppresses type I interferon production by preventing nuclear translocation of phosphorylated IRF3. Int J Biol Sci. 2021;17(6):1547-54.

126. Shemesh M, Aktepe TE, Deerain JM, McAuley JL, Audsley MD, David CT, et al. SARS-CoV-2 suppresses IFNβ production mediated by NSP1, 5, 6, 15, ORF6 and ORF7b but does not suppress the effects of added interferon. PLoS Pathog. 2021;17(8):e1009800.
127. Merad M, Martin JC. Pathological inflammation in patients with COVID-19: a key role for monocytes and macrophages. Nat Rev Immunol. 2020;20(6):355-62.
128. Tan L, Wang Q, Zhang D, Ding J, Huang Q, Tang YQ, et al. Lymphopenia predicts disease severity of COVID-19: a descriptive and predictive study. Signal Transduct Target Ther. 5. England2020. p. 33.
129. Xiong Y, Liu Y, Cao L, Wang D, Guo M, Jiang A, et al. Transcriptomic characteristics of bronchoalveolar lavage fluid and peripheral blood mononuclear cells in COVID-19 patients. Emerg Microbes Infect. 2020;9(1):761-70.
130. Cicchese JM, Evans S, Hult C, Joslyn LR, Wessler T, Millar JA, et al. Dynamic balance of pro- and anti-inflammatory signals controls disease and limits pathology. Immunol Rev. 2018;285(1):147-67.
131. Delogu G, Goletti D. The spectrum of tuberculosis infection: new perspectives in the era of biologics. J Rheumatol Suppl. 2014;91:11-6.
132. Davis JM, Ramakrishnan L. The role of the granuloma in expansion and dissemination of early tuberculous infection. Cell. 2009;136(1):37-49.
133. Joana Da Silva D, Laure D, Antonio P. Exploring the mechanisms of granuloma formation in vivo to prevent dissemination of a respiratory mycobacterium tuberculosis infection: A live imaging approach. European Respiratory Journal. 2016;48(suppl 60):PA2696.
134. Ulrichs T, Kaufmann SHE. New insights into the function of granulomas in human tuberculosis. The Journal of Pathology. 2006;208(2):261-9.
135. Tuvim MJ, Evans SE, Clement CG, Dickey BF, Gilbert BE. Augmented lung inflammation protects against influenza A pneumonia. PLoS One. 2009;4(1):e4176.
136. Kolodny O, Berger M, Feldman MW, Ram Y. A new perspective for mitigation of SARS-CoV-2 infection: priming the innate immune system for viral attack. Open Biol. 2020;10(7):200138.
137. Baker PJ, Amaral EP, Castro E, Bohrer AC, Torres-Juárez F, Jordan CM, et al. Co-infection of mice with SARS-CoV-2 and Mycobacterium tuberculosis limits early viral replication but does not affect mycobacterial loads. Front Immunol. 2023;14:1240419.
138. Hildebrand RE, Chandrasekar SS, Riel M, Touray BJB, Aschenbroich SA, Talaat AM. Superinfection with SARS-CoV-2 Has Deleterious Effects on Mycobacterium bovis BCG Immunity and Promotes Dissemination of Mycobacterium tuberculosis. Microbiol Spectr. 2022;10(5):e0307522.
139. Rosas Mejia O, Gloag ES, Li J, Ruane-Foster M, Claeys TA, Farkas D, et al. Mice infected with Mycobacterium tuberculosis are resistant to acute disease caused by secondary infection with SARS-CoV-2. PLoS Pathog. 2022;18(3):e1010093.
140. Williams BD, Ferede D, Abdelaal HFM, Berube BJ, Podell BK, Larsen SE, et al. Protective interplay: Mycobacterium tuberculosis diminishes SARS-CoV-2 severity through innate immune priming. Frontiers in Immunology. 2024;15.
141. Larsen SE, Reese VA, Pecor T, Berube BJ, Cooper SK, Brewer G, et al. Subunit vaccine protects against a clinical isolate of Mycobacterium avium in wild type and immunocompromised mouse models. 2021.

142. Reuschl AK, Edwards MR, Parker R, Connell DW, Hoang L, Halliday A, et al. Innate activation of human primary epithelial cells broadens the host response to Mycobacterium tuberculosis in the airways. PLoS Pathog. 2017;13(9):e1006577.
143. Escobar LE, Molina-Cruz A, Barillas-Mury C. BCG vaccine protection from severe coronavirus disease 2019 (COVID-19). Proc Natl Acad Sci U S A. 2020;117(30):17720-6.
144. Ten Doesschate T, van der Vaart TW, Debisarun PA, Taks E, Moorlag S, Paternotte N, et al. Bacillus Calmette-Guérin vaccine to reduce healthcare worker absenteeism in COVID-19 pandemic, a randomized controlled trial. Clin Microbiol Infect. 2022;28(9):1278-85.
145. Chu H, Chan JF, Yuen TT, Shuai H, Yuan S, Wang Y, et al. Comparative tropism, replication kinetics, and cell damage profiling of SARS-CoV-2 and SARS-CoV with implications for clinical manifestations, transmissibility, and laboratory studies of COVID-19: an observational study. Lancet Microbe. 2020;1(1):e14-e23.
146. Fogh J, Fogh JM, Orfeo T. One hundred and twenty-seven cultured human tumor cell lines producing tumors in nude mice. J Natl Cancer Inst. 1977;59(1):221-6.
147. Mautner L, Hoyos M, Dangel A, Berger C, Ehrhardt A, Baiker A. Replication kinetics and infectivity of SARS-CoV-2 variants of concern in common cell culture models.
148. Cheemarla NR, Watkins TA, Mihaylova VT, Wang B, Zhao D, Wang G, et al. Dynamic innate immune response determines susceptibility to SARS-CoV-2 infection and early replication kinetics. J Exp Med. 2021;218(8).
149. Moss P. The T cell immune response against SARS-CoV-2. Nature Immunology. 2022;23(2):186-93.
150. dos Santos Alves RP, Timis J, Miller R, Valentine K, Pinto PBA, Gonzalez A, et al. Human coronavirus OC43-elicited CD4+ T cells protect against SARS-CoV-2 in HLA transgenic mice. Nature Communications. 2024;15(1):787.
151. Wang X, Yuen TT, Dou Y, Hu J, Li R, Zeng Z, et al. Vaccine-induced protection against SARS-CoV-2 requires IFN-γ-driven cellular immune response. Nat Commun. 2023;14(1):3440.
152. Hilligan KL, Namasivayam S, Clancy CS, Baker PJ, Old SI, Peluf V, et al. Bacterial-induced or passively administered interferon gamma conditions the lung for early control of SARS-CoV-2. Nat Commun. 2023;14(1):8229.
153. Petrone L, Petruccioli E, Vanini V, Cuzzi G, Gualano G, Vittozzi P, et al. Coinfection of tuberculosis and COVID-19 limits the ability to in vitro respond to SARS-CoV-2. Int J Infect Dis. 2021;113 Suppl 1:S82-s7.
154. Riou C, du Bruyn E, Stek C, Daroowala R, Goliath RT, Abrahams F, et al. Relationship of SARS-CoV-2-specific CD4 response to COVID-19 severity and impact of HIV-1 and tuberculosis coinfection. J Clin Invest. 2021;131(12).
155. Plumlee CR, Barrett HW, Shao DE, Lien KA, Cross LM, Cohen SB, et al. Assessing vaccine-mediated protection in an ultra-low dose Mycobacterium tuberculosis murine model. PLoS Pathog. 2023;19(11):e1011825.
156. Jarde A, Romano E, Afaq S, Elsony A, Lin Y, Huque R, et al. Prevalence and risks of tuberculosis multimorbidity in low-income and middle-income countries: a meta-review. BMJ Open. 2022;12(9):e060906.
157. Jarde A, Siqueira N, Afaq S, Naz F, Irfan M, Tufail P, et al. Correction: Addressing TB multimorbidity in policy and practice: An exploratory survey of TB providers in 27 high-TB burden countries. PLOS Glob Public Health. 3. United States: Copyright: © 2023 Jarde et al. This is an open access article distributed under the terms of the Creative Commons Attribution

License, which permits unrestricted use, distribution, and reproduction in any medium, provided the original author and source are credited.; 2023. p. e0002186.
158. Hertz D, Dibbern J, Eggers L, von Borstel L, Schneider BE. Increased male susceptibility to Mycobacterium tuberculosis infection is associated with smaller B cell follicles in the lungs. Scientific Reports. 2020;10(1):5142.
159. Baldwin SL, Reese VA, Larsen SE, Pecor T, Brown BP, Granger B, et al. Therapeutic efficacy against Mycobacterium tuberculosis using ID93 and liposomal adjuvant formulations. Front Microbiol. 2022;13:935444.
160. Larsen SE, Berube BJ, Pecor T, Cross E, Brown BP, Williams BD, et al. Qualification of ELISA and neutralization methodologies to measure SARS-CoV-2 humoral immunity using human clinical samples. J Immunol Methods. 2021;499:113160.
161. Downs SL, Madhi SA, Van der Merwe L, Nunes MC, Olwagen CP. High-throughput nanofluidic real-time PCR to discriminate Pneumococcal Conjugate Vaccine (PCV)-associated serogroups 6, 18, and 22 to serotypes using modified oligonucleotides. Scientific Reports. 2021;11(1):23728.
162. Kupz A, Zedler U, Stäber M, Kaufmann SH. A Mouse Model of Latent Tuberculosis Infection to Study Intervention Strategies to Prevent Reactivation. PLoS One. 2016;11(7):e0158849.
163. Nemeth J, Olson GS, Rothchild AC, Jahn AN, Mai D, Duffy FJ, et al. Contained Mycobacterium tuberculosis infection induces concomitant and heterologous protection. PLoS Pathog. 2020;16(7):e1008655.
164. Gibbert K, Schlaak JF, Yang D, Dittmer U. IFN-α subtypes: distinct biological activities in anti-viral therapy. Br J Pharmacol. 2013;168(5):1048-58.
165. Liu Y-G, Jin S-W, Zhang S-S, Xia T-J, Liao Y-H, Pan R-L, et al. Interferon lambda in respiratory viral infection: immunomodulatory functions and antiviral effects in epithelium. Frontiers in Immunology. 2024;15.
166. Oleinik LA, Madonov PG, Pykhtina MB. Potential of Interferon Lambda as an Inhibitor of SARS-CoV-2. Mol Biol. 2023;57(2):291-8.
167. Syedbasha M, Egli A. Interferon Lambda: Modulating Immunity in Infectious Diseases. Frontiers in Immunology. 2017;8.
168. Sposito B, Broggi A, Pandolfi L, Crotta S, Clementi N, Ferrarese R, et al. The interferon landscape along the respiratory tract impacts the severity of COVID-19. Cell. 2021;184(19):4953-68.e16.
169. Reis G, Silva EASM, Silva DCM, Thabane L, Campos VHS, Ferreira TS, et al. Early Treatment with Pegylated Interferon Lambda for Covid-19. New England Journal of Medicine. 2023;388(6):518-28.
170. Chong Z, Karl CE, Halfmann PJ, Kawaoka Y, Winkler ES, Keeler SP, et al. Nasally delivered interferon-λ protects mice against infection by SARS-CoV-2 variants including Omicron. Cell Rep. 2022;39(6):110799.
171. Travar M, Vucic M, Petkovic M. Interferon lambda-2 levels in sputum of patients with pulmonary Mycobacterium tuberculosis infection. Scand J Immunol. 2014;80(1):43-9.
172. Schneider WM, Chevillotte MD, Rice CM. Interferon-stimulated genes: a complex web of host defenses. Annu Rev Immunol. 2014;32:513-45.
173. Li J, Ding SC, Cho H, Chung BC, Gale M, Jr., Chanda SK, et al. A short hairpin RNA screen of interferon-stimulated genes identifies a novel negative regulator of the cellular antiviral response. mBio. 2013;4(3):e00385-13.

174. Schoggins JW, Wilson SJ, Panis M, Murphy MY, Jones CT, Bieniasz P, et al. A diverse range of gene products are effectors of the type I interferon antiviral response. Nature. 2011;472(7344):481-5.
175. Chatterjee S, Nalla LV, Sharma M, Sharma N, Singh AA, Malim FM, et al. Association of COVID-19 with Comorbidities: An Update. ACS Pharmacol Transl Sci. 2023;6(3):334-54.
176. Ng WH, Tipih T, Makoah NA, Vermeulen J-G, Goedhals D, Sempa JB, et al. Comorbidities in SARS-CoV-2 Patients: a Systematic Review and Meta-Analysis. mBio. 2021;12(1):10.1128/mbio.03647-20.
177. Kreutmair S, Kauffmann M, Unger S, Ingelfinger F, Núñez NG, Alberti C, et al. Preexisting comorbidities shape the immune response associated with severe COVID-19. J Allergy Clin Immunol. 2022;150(2):312-24.
178. Chaturvedi R, Lui B, Aaronson JA, White RS, Samuels JD. COVID-19 complications in males and females: recent developments. J Comp Eff Res. 2022;11(9):689-98.
179. Yorke E, Atiase Y, Akpalu J, Sarfo-Kantanka O, Boima V, Dey ID. The Bidirectional Relationship between Tuberculosis and Diabetes. Tuberc Res Treat. 2017;2017:1702578.
180. Ayelign B, Negash M, Genetu M, Wondmagegn T, Shibabaw T. Immunological Impacts of Diabetes on the Susceptibility of Mycobacterium tuberculosis. J Immunol Res. 2019;2019:6196532.
181. Bothamley GH. Male Sex Bias in Immune Biomarkers for Tuberculosis. Front Immunol. 2021;12:640903.

APPENDIX A. SUPPLEMENTAL DATA PERTAINING TO CHAPTER 2

A.1 Flow gating strategy

Supplemental gating strategy may be downloaded from: https://doi.org/10.3389/fimmu.2024.1424374

A.2 Measured lung cell populations counts over time

Supplemental cell population data may be downloaded from: https://doi.org/10.3389/fimmu.2024.1424374

A.3 Primers used for in vivo RT-qPCR

Supplemental primers may be downloaded from: https://doi.org/10.3389/fimmu.2024.1424374

A.4 Kinetic lung mRNA expression of inflammatory-related genes from each mouse infection group

Supplemental expression data may be downloaded from: https://doi.org/10.3389/fimmu.2024.1424374

A.5 Patient information from collected human PBMCs

Supplemental information may be downloaded from:

https://doi.org/10.3389/fimmu.2024.1424374

A.6 Primers used for in vitro RT-qPCR

Supplemental primers may be downloaded from:

https://doi.org/10.3389/fimmu.2024.1424374

APPENDIX B. SUPPLEMENTAL DATA PERTAINING TO CHAPTER 3

B.1 CMTB and SARS-CoV-2 Survival Curve

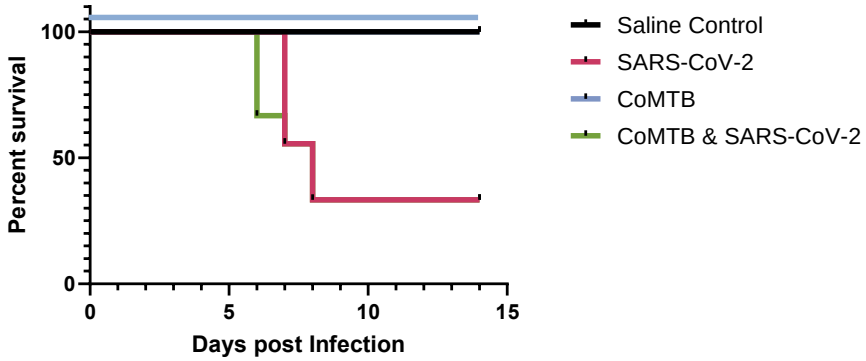

Figure B.1. *CMTB and SARS-CoV-2 Survival Curve. Survival analysis of female infection groups with 10 mice per group). Mouse weights (n=10/group) were recorded daily, and percent weight change calculated from the maximum recorded weight.*

B.2 Survival Over Time

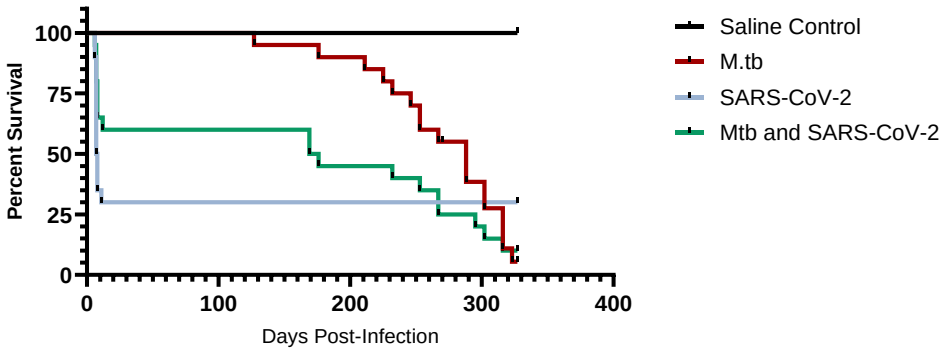

Figure B.1. Survival over time. Survival analysis of female infection groups with 10 mice per group). Mouse weights (n=10/group) were recorded daily, and percent weight change calculated from the maximum recorded weight.